Fall 12-20-2017

Investigation of 2195 and 2219 Post Weld Heat Treatments for Additive Friction Stir Lap Welds

Matthew Champagne
University of New Orleans, mschamp1@uno.edu

Investigation of 2195 and 2219 Post Weld Heat Treatments for Additive Friction Stir Lap Welds

A Thesis

Submitted to Graduate Faculty of the
University of New Orleans
in partial fulfillment of the
requirement for the degree of

Master of Science
in
Engineering
Mechanical

by

Matthew Champagne
B.S. Louisiana State University, 2010
M.S. Louisiana State University, 2013

December 2017

Acknowledgments

First and foremost, I need to thank both Dr. Paul Schilling and Dr. Michael Eller as mentors and advisors on this thesis. They introduced to the world of engineering and made my time at the University of New Orleans more than just about the degree but about finding a new passion. Their patience, guidance, and support made this thesis possible. I also need to thank Anne Marie Joyce for lending me her experience and teaching me the finer details of working in the Metallography lab. I must express my gratitude William Miller Jr., who made polishing samples look easy, for taking the time to impart some of his knowledge to me.

In addition to Dr. Paul Schilling and Dr. Michael Eller, I would like to thank Dr. Paul Herrington, my committee members, for their patience and flexibility and comments during my thesis defense.

I would like to thank Dr. Michael Eller, the University of New Orleans Mechanical Engineering Department and the National Center of Advanced Manufacturing for the teaching assistantship.

I have to express my deepest gratitude to my family and friends who advised me, pushed me, and supported me throughout this entire process. Whenever I would feel discouraged, stressed, or overwhelmed, they were all there to help me and motivate me to push through.

Finally, I want to dedicate this thesis to my fiancée, Lindsey Harvey. She dealt with all the delays and difficulties I had in finishing this project. She encouraged me and motivated me to keep working. This thesis is as much for her as it is for me.

Table of Contents

List of Tables

List of Figures

Figure **Page.**

Abstract

To evaluate potential uses for friction stir welding in additive manufacturing, two separate parts were fabricated, one of 2195-T84 and the other 2219-T87, utilizing fixed pin techniques and additive lap welds. The parts were cut into samples, artificially aged and subjected to Rockwell hardness (HRB), Vickers hardness, micrographic photography, and metallographic imaging on both pre- and post- heat treatment. Additionally, tensile testing was performed on the heat-treated samples. A comparisons of test results showed a minimal increase in the yield strength of the 2195-T84 samples compared to as-welded tensile results obtained from a previous project. The ultimate tensile strength was reduced by approximately 16%. Further testing will be required to determine the nature of this reduction. No previous results were available for the as-welded 2219-T87, but UTS of the artificially aged samples was approximately 91% that of the parent material.

Keywords: Friction Stir Welding; Additive Manufacturing; Al 2195; Al 2219; Al Heat Treatment

Chapter 1: Introduction

1.1 Introduction and Background

As technology and industries move forward and advance, so must the manufacturing techniques associated with and which support those industries. Manufacturing, in general, refers to the creation of a product on a large scale and through the use of machinery. This encompasses a large variety of products, machines, and techniques; each of which are best suited to a given task. Every project must be meticulously designed, and each part fabricated using the most practical techniques available. The advent of friction stir welding (FSW) in 1991 by the Welding Institute of Cambridge in England added another option for manufacturing [1]. FSW is a solid-state process that can be used to join metal parts by creating a metallurgical bond.

Friction stir welding is an autogenous, solid-state welding technique that takes advantage of frictional heating to plasticize metal around a specially designed pin tool. Although FSW can come in several forms, the principle is ultimately the same no matter the variant. The pin tool generally consists of a probe that protrudes from a shoulder as shown in Figure 1. The probe is inserted into sample to be welded, whether that be through a predrilled hole or by using the pin tool to bore a hole to the depth of the shoulder. Once the shoulder is in contact with the surface, the combination of the vertical and rotational forces applied by the pin tool use frictional heating to plasticize the material in the immediate vicinity of the probe. The probe creates a flow of plasticized metal around itself, mixing the materials from the individual parts. The area of flow around probe is known as the extrusion zone. Once the initial material is plasticized, the tool will translate along the weld path. This forward motion along with applied forces will heat the area in

front of the tool so that the material will be appropriately plasticized as it enters the extrusion zone. In addition to providing the frictional heat required for the welding process, the trailing end of the shoulder reforges the material as it leaves the leaves the extrusion zone helping to fully consolidate the material. This has added benefit of putting some of work back into the system that is removed during the welding process.

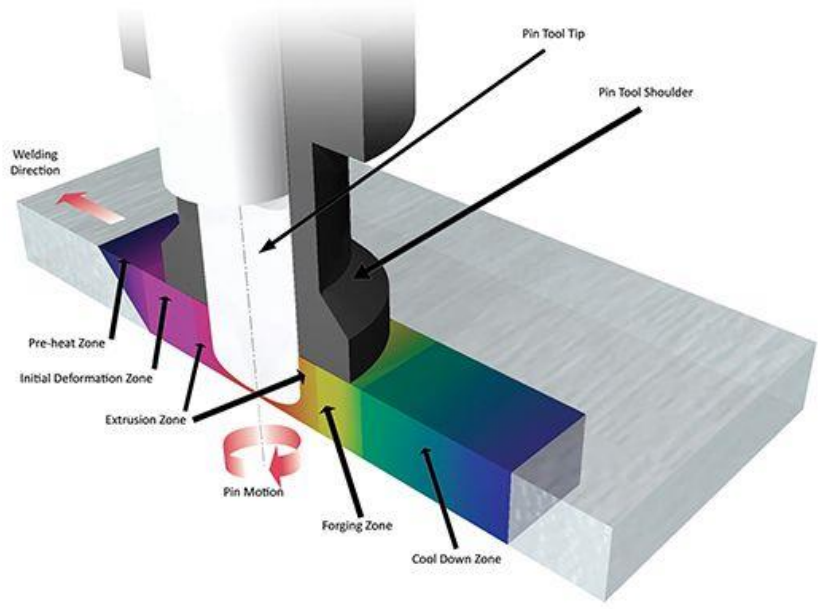

Figure 1: The processing zones created as the pin tool translates along the weld [36].

Friction stir welding can be a complicated process, but has several advantages over traditional welding techniques:

- Better mechanical properties (i.e. strength, lack of deformation, etc.)
- No need for consumables such as welding rods or toxic gasses
- Once a weld schedule is developed, the process can be easily automated producing consistent welds.

Although friction stir welding can produce quality, cost effective welds, the cost of initial setup and weld development can be expensive. Even with the difficulty of the initial cost, friction stir welding has already begun to make its way into modern manufacturing applications.

Fabrisonic is a company that uses state of the art metal printing processes (Ultrasonic Additive Manufacturing or UAM) to create products using solid-state manufacturing processes. In conjunction with their existing processes, UAM and CNC machining, Fabrisonic uses friction stir welding to bridge the gap in the shortcomings of their existing methods. They claim they can use UAM to create solid-state printed fluid channels. UAM alone leaves weak points in the channel ceiling since UAM requires high pressure that the channel cannot support. Using a custom insert and friction stir welding, Fabrisonic is able to produce a heat exchanger produced through solid-state manufacturing. [3]

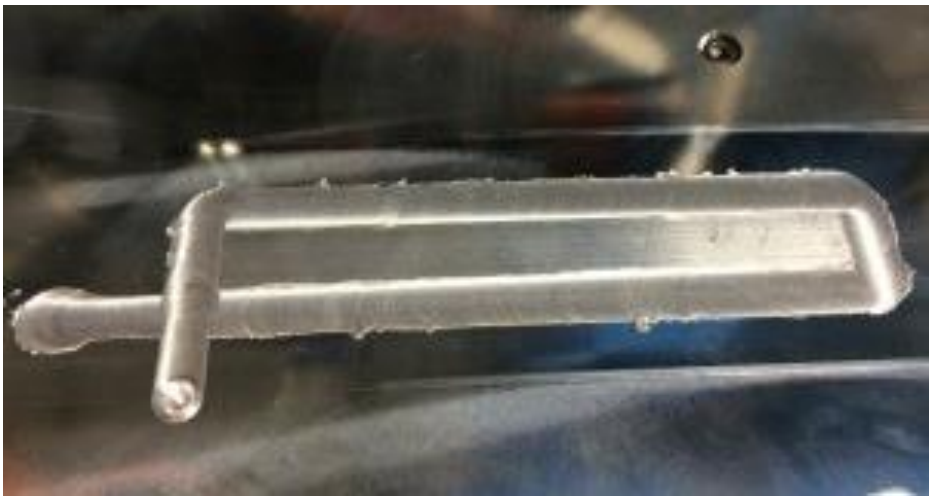

Figure 2: Fabrisonic's use of friction stir welding in combination with ultrasonic additive manufacturing to create solid-state manufactured heat exchangers. [4]

The National Aeronautics and Space Administration (NASA) has been researching the feasibility of friction stir welding for a great number of uses since the mid 90's [5]. The studies led to the extensive use of friction stir welding in the manufacture of the External Tanks used for shuttle missions. Frictions stir welding's ability to be easily controlled, the minimal process

variances, and the increase in joint strength allowed NASA to replace traditional fusion welding with FSW [6]. Since the first uses with the External Tanks, NASA has gone on to incorporate FSW into many of its designs including the extensive use on the Orion project [7].

Figure 3: Seen here is the first weld of the Orion crew module (ground test module) done by Lockheed Martin using the Universal Weld System II (UWSII) at the Michoud Assembly Facility. [8]

The use of FSW has also expanded into the marine vessel industry. The use of aluminum hull ships can significantly reduce the weight of vessels allowing for greater fuel efficiency, low draft vessels, and the ability to care a more cargo. In addition, FSW allows for the use of corrosion resistant materials such as 5000 and 6000 series aluminums. The use of these materials extends the lifespan of the vessels. Tamano Works of Mitsui Engineering and Shipbuilding (MES) of Japan has applied FSW practices to its passenger and freight liner the “Super Liner Ogasawara,” which can be seen in Figure 3. The vessel is capable of carrying 740 persons and 210 tons of freight. [9]

Figure 4: The Super Liner Ogasawara built by. Tamano Works of Mitsui Engineering and Shipbuilding (MES) of Japan has incorporated friction stir welding into the manufacturing process.

1.3 Friction Stir Welding

The Welding Institute of Cambridge started with a simple process that included a rotating shoulder with a protruding probe [1]. FSW has become a much more sophisticated process thanks to research along with advances in materials, tools, and machining. incorporating variations in tooling type and design, advances in machinery, and materials. Additionally, the use of multiaxis machines allows for complex 3-dimensional welds. Advances in materials and research into the weldability of existing materials have also led to steady increase in applications of FSW for a variety of industries as discussed previously.

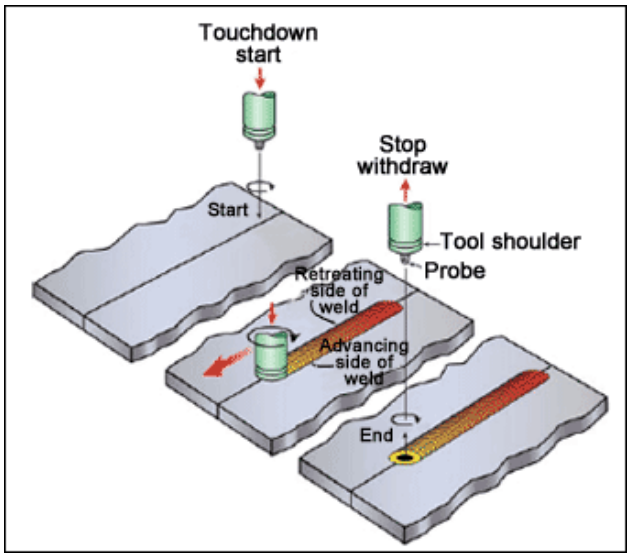

Figure 5: Friction stir welding utilizes a combination vertical and rotational forces applied through the pin to plasticize the material. As the pin tool advances, the plasticized material is forced to flow around the tool combining the material from the separate components of the weld. The plasticized metal is reforged by the shoulder as it translates along the weld. [35]

Three distinct variations of friction stir welding have emerged as the predominant techniques, each of which have their own tooling and applications: fixed pin, adjustable pin, and self-reacting. The fixed pin variation uses a tool with a pin in a fixed position in reference to the shoulder. Fixed pin can work well but can leave large holes in the welded materials at the end of the weld. The adjustable pin method utilizes a pin that can be extended and retracted separately from the shoulder. This allows for the pin the shoulder to start flush with the base materials and retracted over a distance. This helps remove the problem of a hole the size of pin tool at the end of the weld. The self-reacting welding method utilizes two shoulders, one above the weld and one below the weld. Instead of the force being applied by a single shoulder, the majority of force is applied between the two shoulders connected by the pin. Self-reacting welds creates a weld entirely through a sample along with a large weld nugget.

Although most friction stir welding applications employ the previously described methods, an alternative method known as stationary shoulder or static shoulder friction stir welding has

shown some promise. Stationary shoulder friction stir welding (SSFSW) utilizes a probe rotating through a stationary shoulder. Traditional FSW uses significant forge loads along with rotational speeds generally ranging from 200 rpm to 1,500 rpm to generate frictional heating. SSFSW utilizes rotational speeds between 2,000 rpm and 10,000 rpm to generate the frictional heat that plasticizes the welded material, which requires a much lower forge force since the shoulder is no longer generating the majority of the heat. Additionally, the high speeds also produce a much larger stir zone around the pin tool creating a more substantial weld nugget. [42]

1.2.2 Butt weld configuration

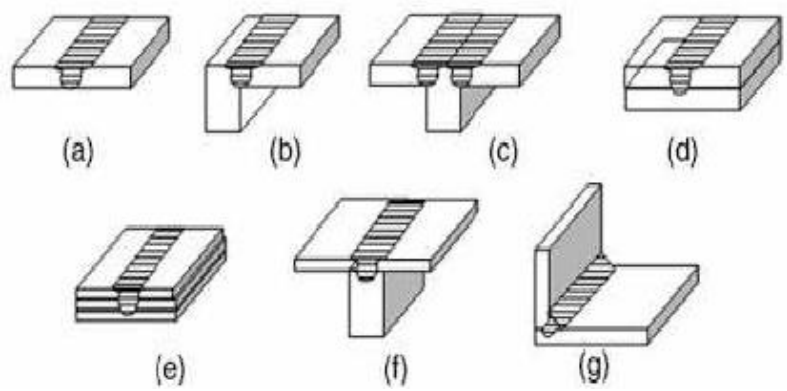

Figure 6: The seven basic weld variations [11]

Each of the variations of friction stir welding has their own distinct advantages and disadvantages. When a part is being designed, it is important to carefully examine the configuration and determine which type of FSW is best suited for the desired for the project. Although weld designs can be complex and unique, they can generally be simplified and classified as variations of seven basic weld configurations. [11]

The basic weld, known as butt weld (Figure 6 a), consists of two pieces of material butted together. Depending on the application, all three variations of FSW can be applied to the butt weld. Fixed pin FSW can be used to create a uniform weld, but has several draw backs in this case. Although fixed pin FSW will join the panels, the weld will not fully penetrate the joint. It will also

leave a hole at the end of the weld where the probe is removed, also known as the keyhole. Adjustable pin will minimize the issues caused by the abrupt removal of the probe associated with fixed pin, but will still be unable to fully join the panels. Self-reacting FSW is often best suited for butt welds since it can weld the entire joint, but will either leave tear at the exit or leave a keyhole that will require attention. Other work has been done to rectify issues caused by the void left at the end of the weld using a process known as friction plug welding [12].

Additionally, two variations of the simple butt weld exist in common designs. The edge butt consists of the vertical edge of a plate butted against the horizontal edge of the second piece of material (Figure 6 b). The T butt weld is a variation on edge butt joint (Figure 6 c). It consists of a second horizontal piece of material butted on the opposite side of the first horizontal part creating a T formation. These configurations lend themselves to both fixed and adjustable pin welds, but still have the same issues that come with simple butt weld.

1.2.3 Lap weld configuration

Although butt welds the most common, FSW is well suited performing the second major configuration, the lap weld. The simple lap joint consists of a single plate lain on top a another and welded together through the upper panel (Figure 6 d). This weld creates a metallurgical bond between these two plates in the welded areas. Friction stir welding has a distinct advantage over traditional welding techniques in this joint configuration. Traditional welding does not have the capacity to weld through one plate into another without filler material and traditional is only used to overlap the ends of two plates. Whereas, FSW can be bond the panels essentially anywhere the two plates are overlain.

Similar to the simple lap joint, the multiple lap joint consists of multiple plates overlain and welded through the top plate and the center plate or plates into the bottom plate (Figure 6 e),

while the T lap weld consists of butt weld centered over a third plate placed perpendicular to the other two plates (Figure 6 f). Fixed pin and adjustable pin FSW are traditionally used for lap welds although in theory self-reacting FSW can be used for the simple lap and multiple lap joints. It should be noted that there is a seventh join configuration, the fillet joint, which consists of 90° joint welded from the interior (Figure 6 g).

1.4 Weld Zones, Defects and Artifacts

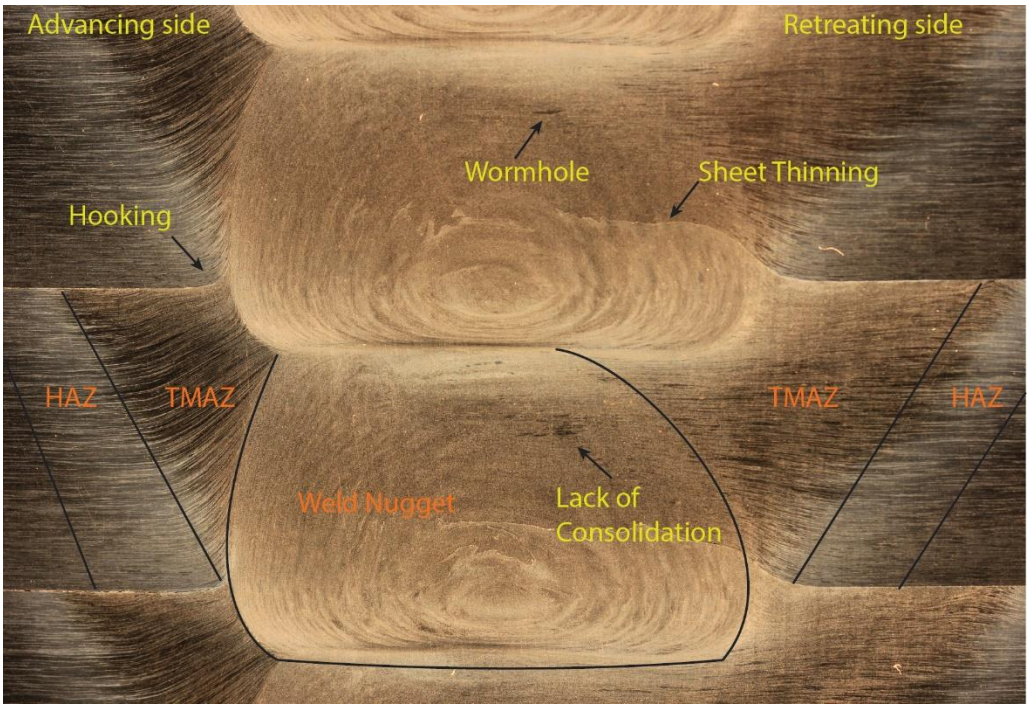

Figure 7: Typical cross section of 2195-T84 weld with zones and defects labeled

At its simplest, friction stir welding is a process that uses primarily a combination of forces to apply heat and stress to a sample. This obviously will influence the grain structure of the area within the weld that has been plasticized and reforged. As the material is plasticized, the initial grain structure is destroyed. The vertical load applied by the shoulder serves to reforge the material as well as ensure that the material is well consolidated. This creates a very fine grained section of material that is at the heart of weld, the stir zone or weld nugget. Due to the fact that the pin tool

is both translating and rotating, the resultant weld nugget is non-symmetric. The boundaries between the different zones are much less well defined on the retreating side. The area just outside the weld nugget will still experience both the force and heat caused by the process and will experience some plastic deformation, but does not fall under the influence of the extrusion zone. The area is known as the thermo-mechanical zone (TMAZ). The area adjacent to the TMAZ will still experience a sizable amount of heat, but it is beyond the influence of the applied forces. The heat essentially acts as an annealing process, which will affect the microstructure, but this heat affected zone (HAZ) will not undergo any plastic deformation. The area beyond the HAZ the material is unaffected by the weld is simply the parent material.

When viewing the cross section of the weld, it is important to understand the asymmetry experience in the weld nugget is also seen in each of the other weld zones. The "advancing side" is the side that the rotation and translation are aligned. It is usually characterized by very well-defined boundary between the nugget and the TMAZ and the TMAZ and the HAZ. The "retreating side" is that in which the translation and rotation are in opposite directions. The zone boundaries can be much more difficult to define on the retreating side.

As with any weld, the process is not always perfect, and several defects can influence the overall quality of the final weld. When evaluating a weld often the most obvious defect would be a wormhole, or a void in the cross section of the weld. Wormholes, as seen in Figure7, can be the result of several different issues especially a lack of forge force and to little or excessive rotational speeds. A variation of the wormhole is the surface lack of fill as seen in Figure 8, and is largely caused by the same issues associated with wormholes, but is more influenced by the forge force.

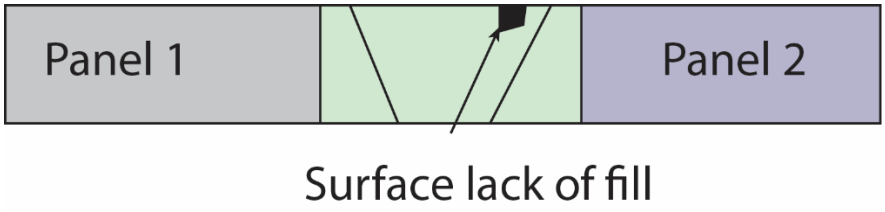

Figure 8: Surface lack of fill

A cold lap or kissing bond defect is a little less common than the previous two and much more difficult to find. It consists of an oxide layer at the faying edge that was not appropriately broken up during the welding process. The oxide layer prevents or at least limits metallurgical bonding. [8]

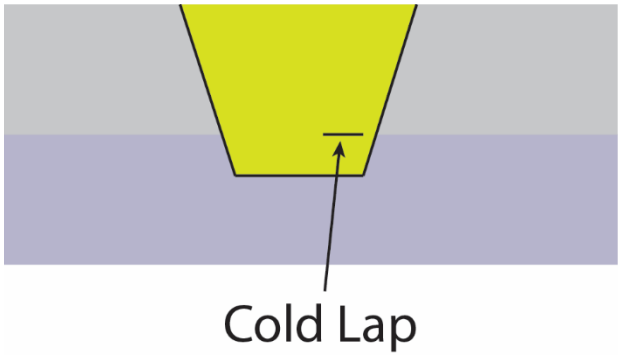

Figure 9: Cold Lap

Not all visible features are considered defects though. Hooking and thinning are considered to be weld artifacts. In general, they do not affect the overall strength of the material, although it does in some loading conditions. Hooking and thinning occur when the pin tool induces a vertical flow. As seem in Figure 7, the pin tool's will force the panel interface to flow. Hooking generally occurs on the advancing side. Sheet thinning generally is encountered on the retreating side. The pin tool's flow essentially pulls the interface into weld nugget. In doing so thickness of the affected panel (sheet) is reduced.

1.5 Additive Manufacturing

Figure 10 Near net shape part manufactured at Cranfield University using wire arc welding.

The design of a fabricated part can be a complicated process that must consider not only the components use, but the manufacturing process required along with the cost to produce it. The relatively new field of additive manufacturing (AM) is helping to change the way industries work by producing complicated parts with minimal loss. The most widely known type of process in the field of AM has become 3D printers. The advent of 3D printers can be traced back to research done as far back as the 1970's. The first patent was issued to Dr. Kodama in 1981 for his rapid prototying machine which utilized layered photopolymers to build cost-effective prototypes [38]. This initial process was great for making prototypes, but not for full scale manufacturing. As the years progressed, additional techniques such as stereolithography and sintering helped to advance

the field. Additive manufacturing is constantly evolving and advancing to allow for more precise parts to be fabricated from a wide range of materials. Most machines still utilize various plastics or resins to form parts. The use of these materials in additive manufacturing limits field of applications. The expansion of additive manufacturing into metallic materials has led to the advent of many techniques.

Fabrication in traditional manufacturing generally starts with a single block of material, which is then machined down to individual components in a process known as subtractive manufacturing. This process can often be labor intensive, expensive, and lead to significant material waste. In contrast, additive manufacturing forms a part by layering material to form a component or the near net shape of a component. This is most often done by taking a 3D design and breaking it down into 2D cross-sections of a with a given thickness. The part begins with the base cross-section and is then build up by adding each consecutive layer until the component has been completed. Various plastics and resins are great for this type of manufacturing due to the low melting point of the material. Although using these technologies complex plastic components can be easily fabricated, the functionality of the parts is limited by the low strength and durability of the parent material.

Using metals to produce higher strength fabrications makes the process significantly more difficult. Most metal AM technologies can be broken down into three categories: powder bed, powder fed and wire. Powder bed systems use a thin layer of metal powder even raked over a flat bed. A laser or electron beam guided by the computer system is then used to melt or sinter the powder. As each layer is finished a new layer of powder is raked over the work surface and the process is repeated until the final part has been made. Powder fed systems utilizes a focused laser to deposit powder that is fed to the system from and external supply. Finally wire fed systems can

use a variety of energy sources such as a laser, electron beam, or plasma arc to melt a metallic wire as it is placed into the fabricated product. This creates a near net shape which will require additional machining to achieve the final component [39]. An example of a wire fed part can be seen in Figure 10.

Although current additive manufacturing processes have many advantages, such as being able to create complex parts at no additional cost, the relative minimal skill required compared to traditional fabrication and speed with which a part can be made, these techniques also have several disadvantages. The machines required for AM are often expensive and require high energies. Additionally, components are limited in size due to the machine's constraints. Larger parts require larger, more expensive machines. Finally, the mechanical properties of the finished component are often diminished as a result of the process due to increased porosity, multiple melt interfaces and variations in grain size and alloy component melting temperatures. Some of these issues can be minimized through additional heat treatments, but the AM is still limited by these constraints.

1.6 Aluminum 2195 and 2219

Although aluminum can come in a great many variety of alloys, each of which is often tailored for specific uses. A distinction must first be made between the two major classes of aluminum. Cast aluminum alloys are those that are directly cast into the final shape or near final shape without ensuing work or machining. Wrought aluminum generally refers to a product that has been produced in an ingot form and is subsequently worked through exuding, rolling, forging, or other metal working process before being used to create a final product. When a new wrought aluminum alloy is created, it is given a specific four-digit number that is used to describe it (cast aluminum has a separate numbering system). The initial number is one through eight, characterizing the major alloying metal, i.e. 7XXX is generally uses Zinc as the primary alloying

agent. The second relates information about how many times the specific series has been modified, with 0 being the first iteration. The final two digits identify the specific alloy within the series. The exception is the 1000 series (pure aluminum) in which the final two digits represent the minimum purity of the Al.

In addition to the four digit number system, many alloys will be given a designation after alloy number like 2195-T84. This designation gives information about the temper of alloy. The temper can be very important when choosing an alloy for friction stir welding and will be discussed more below. This thesis focuses on two alloys, Aluminum 2195-T84 and 2219-T87. These are both aluminum-lithium alloys, which are known for their high strength to weight ratio. This higher than usual strength to weight ratio is useful when you need high strength, but cannot sacrifice the weight required to use stronger alloys, such as most 7000 series aluminum or steel. 2000 series Al has become popular in Aerospace and aeronautical industries due to advantageous properties including its strength to weight ratio and weldability.

1.7 Temper and Post Weld Heat Treatment

As discussed in Section 1.5, the chemical composition of an aluminum alloy helps determine the mechanical properties. Additional work, heat treatment, and/or stress relief after initial fabrication can also affect the ductility, strength, weldability etc. of the alloy. These process, which are used to optimize the material properties, are described by the Aluminum Association Alloy and Temper Designation System. The designation system has five basic categories to describe the temper of a given material: as fabricated (-F), annealed (-O), strain hardened (-H), solution heat treated (-W), and thermally treated (-T).

Annealing, as designated by the -0 temper, is a low temperature heat treatment that can be used to remove internal stresses, recrystallize grained deformed by internal stress, and increase

grain size. Although annealing generally results in a softer, weaker material, the reduction in internal stresses creates a more workable material. The annealed state is generally the lowest strength temper. The solution heat treated condition (-W) is applied to aluminum alloys that have been thermally treated in the presence of a solution whose constituents will enter a solid solution within the material. When the material has been quenched it will form a supersaturated state that will help the material age harden.

Products that primarily gain additional strength through cold work are considered strain hardened (-H). Although strain hardening can be used to increase the strength, it also increases the brittleness of the material. When a product is strain hardened, the designation is always followed by one or more numbers the indicate the specific processes used on material and the amount of strain imparted on the material. The H1 temper is given to an alloy that has only undergone strain hardening to achieve the desired level of strength. H2 indicates that the strain hardened material has been partially annealed to reduce its strength to the desired amount. H3 refers to metals that have undergone thermal stabilization, increasing ductility, in materials that age soften at room temperature. Stabilization can either occur during the fabrication process or as a low temperature treatment after the material has been worked. The final basic designation is the H4 temper, which indicates that the final product has been subjected to heat during a painting or lacquering process. The second digit in the temper designation always indicates the minimum value of the tensile strength after the alloy has been fabricated.

The final designation (-T) is given to products that have undergone some other heat treatment than the previous designations (-0, -W, or – H). As with the -H tempers, the first digit indicates the specific combination of operations undergone. The designation from 1 to 10 indicates a specific combination of cooling, solution heat treatment, cold work, natural and artificial aging,

and stabilization. The parent materials used for this thesis began with the T8 temper, which indicates that the material has been solution heat treated, cold worked, and then naturally aged. Friction stir welding is an elevated temperature shaping process, whose forge force imparts some strain into the system. This thesis utilizes artificial aging to help form uniform grains and increase the strength within the weld nugget.

Chapter 2: Experimental Setup

2.1 Weld and Fixture Design

Figure 11 The welding fixture was designed to create a simple part in which a single linear part could be machined and tested to determine the mechanical properties.

Friction stir welding has grown to have a well-respected and defined place in the manufacturing toolbox, but also has unexplored potential for uses in additive manufacturing. The goal of this thesis is not to create a working part, but to evaluate the feasibility of using friction stir welding for additive manufacturing. To that end, both the fixture and weld were specifically designed to create a component that will lead to a better understanding of the capacity of friction stir welding for use in additive manufacturing.

The weld consists of sixteen (16) 2 inch by 12 inch by 0.255 inch panels of virgin aluminum alloy individually lap welded. The panels were initially cut to size using a band saw from 4 inch by 24 inch by 0.255 inch factory machined plates. The initial weld was performed using two virgin panels joined by a lap weld along the 2 inch face using a fixed pin friction stir weld. Another layer is then added by welding a third panel on top of the previous weld. This process is repeated until

the desired height is achieved, in this case approximately 4 inches. To accomplish this goal, a welding fixture was designed to maintain panel position and stability while creating a sizable heat sink.

The fixture, as seen in Figure 11, consisted of a base steel plate containing several threaded holes. To keep a consistent coordinate system and provide a heat sink, a 4-inch-thick steel block with even spaced threaded holes was attached to the base along with a backstop for the plates. This created a 90-degree corner that allowed the machined edges of the cut specimens to be aligned and to maintain contact with the heat sink. In addition to the heat sink and backstop, a set of bars was placed approximately 3 inches from the heat sink creating a 3 inch wide by four inch high gap to hold the individual panels. A series of side clamps were installed into the guide bars both to keep the cut panels from moving laterally and to keep the machined edges of the plates flush as each of the welds were performed.

A single lap weld can be broken down into three components: the plunge, the weld and the pin removal. The trial runs included determining the optimum parameters for both the plunge and the weld. To minimize the variations in weld parameters, the end of the weld was only considered to the extent that the pin tool was not damaged. The initial feasibility of this welding process was done through the National Center of Advanced Manufacturing (NCAM), in a class taught by Michael Eller, Ph.D., who also designed the fixture. The weld parameters, forge force, rotation speed, and translation speed were determined through a combination of experience with the materials and several trial runs on a single lap weld.

In a fixed pin friction stir weld, the plunge phase is as important as the weld itself, and great care must be taken to determine the optimal machine settings to complete a quality weld. The plunge must include a high enough rotational speed to bore a hole into the material, a slow

enough plunge rate as to not damage the pin tool, and enough force and time to plasticize the material. The initial phase of the trials included multiple plunge attempts, each with varied parameters. The optimal plunge was chosen according to the above criteria by visually inspecting dwell process along with the resulting void and cross-section.

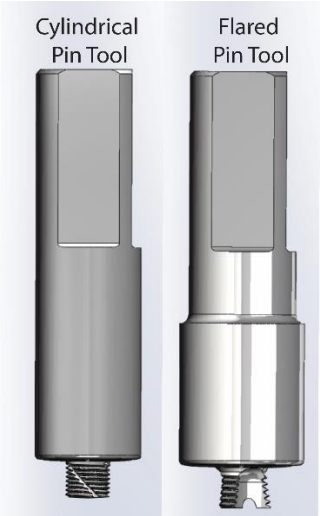

Figure 12: The two types of pin tools used in the weld trials and the NCAM FSW class. The cylindrical pin can be seen on the left and the flared on the right.

Once the initial plunge parameters were obtained, the translational weld parameters were determined again through trial and error. Starting with conservative parameters (higher forge force and slower translation) as to not damage the pin tool, a short linear lap weld was performed (approximately 2 inches). Several short welds were performed varying the weld parameters to help reduce the undesired effects of the weld: flashing, the pin tool digging into the surface, excessive scroll marks, etc. The welds with the most potential were then cut into approximate one inch cubes using a band saw. Finally, the samples were polished, etched and evaluated using macrographic photography. Taking into account the effect on the surface and defects in the cross-section, the welds with the most potential were chosen for the class project. In addition to determining the weld parameters, the trials were run using two types of pin tools, a cylindrical pin and a flared pin as

seen in Figure 12. The cross-section of lap welds produced by the cylindrical and flared pins as seen in Figure 13. All trials we performed on 2195-T84.

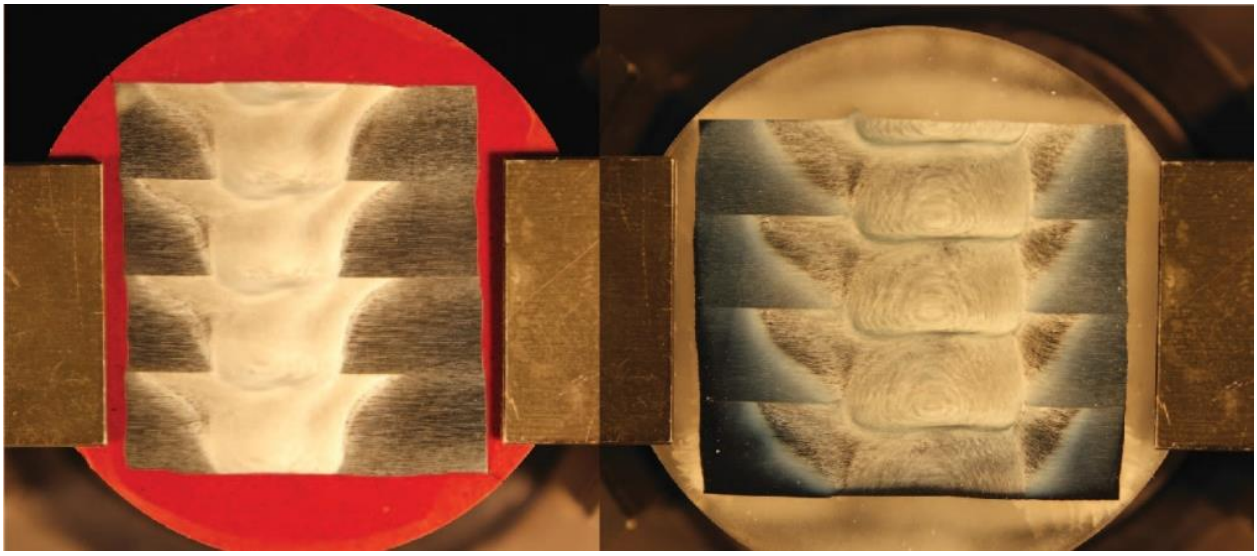

Figure 13: Comparison between cylindrical pin weld and flared pin weld

Although the class determined the initial feasibility of stacked lap welds, testing was limited due a reduced scope used for teaching and time constraints. The front end of the fabricated part was cut just after the dwell location and just before the end of the weld, both of which were reserved for polishing. The main section of each of the weld stacks were fly cut into panels, each approximately 0.25 inches thick centered on the weld. The class panels were cut into six (6) individual coupons and machined to ASTM standard for tensile testing. the panels produced as part of this thesis were cut into eight (8) coupons. The entire process from the raw panels through producing the coupons has been outlined in Figure 14. All tensile tests were run according to ASTM E8. The results of the tensile tests are presented in Chapter 3.

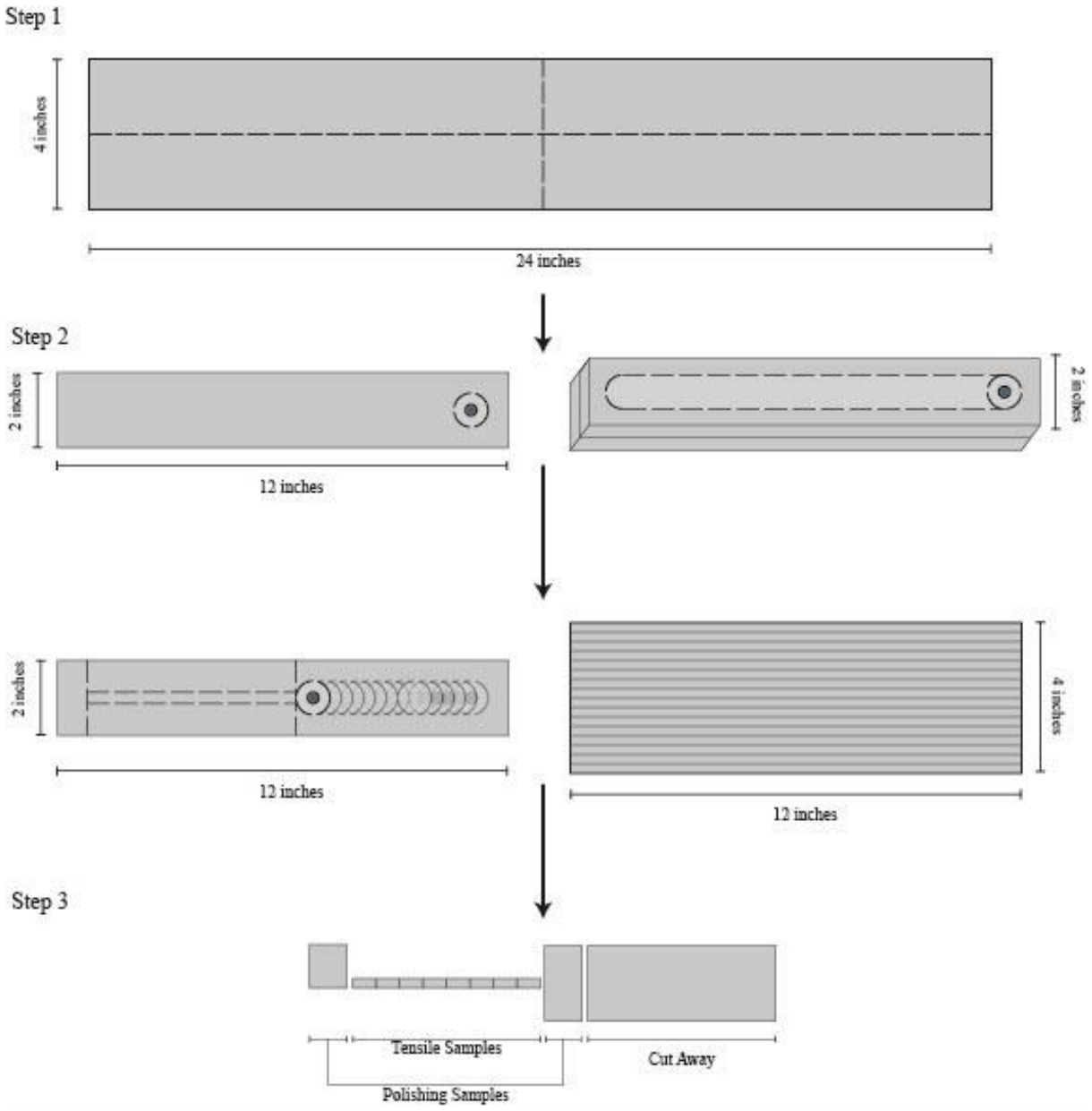

Figure 14: The final component started as four 4 inch by 24 inch panels which were cut, welded, and machined for testing.

Taking into account the results of the feasibility project performed as part of the NCAM class, this thesis focuses on evaluating the effect of heat treatment of the stacked lap welded components. Using the flared pin tool, a part was fabricated using the optimal parameters previously discussed. As an additional comparison, a second component was made using 2219-T87 using similar weld parameters as 2195-T84 with minor changes to the to make to the welds

more suitable to the material. Each component was subjected to a series of tests to evaluate the change in mechanical properties as a result of the heat treatment.

2.2 Heat Treatment

The advantages of heat treatments were previously discussed in section 1.7. Although the advantages of heat treatments in both aluminum alloys and friction stir welds are well documented and capable of optimizing mechanical properties, the goal of this thesis was not to determine the optimal characteristics for each weld. The primary objective was to determine feasibility of heat treatments for this weld configuration. It also serves a secondary goal of a benchmark for future work.

The heat treatment used was chosen considering previous work done on similar materials [25,26] and techniques [27]. Although there is very little literature on heat treatments of Al 2195, Stephen Hales' work on post weld heat treatments and quenching practices on post-super plastic formed X2095, an early version of 2195, [13] was used as a basis for understanding the effect of post weld heat treatment on friction stir welded 2195. Hales' work showed that once peak aging has been reached, elongation can be significantly reduced. Although strength can be maximized, it is often important to balance the benefits of higher strength and the reduction in elongation.

This thesis studies and compares the effects of post weld heat treatment on both Al 2195 and Al 2219 of the friction stir weld nugget of continuous lap welds. Since no work has been done in this regard previously, a basic heat treatment was used to help both determine feasibility and establish a baseline for future comparison. The welded panels initially cut into the rough coupons for conducting tensile tests and samples to be polished. After initial tests described in section 2.3 were performed, the samples were placed in a room temperature furnace and heated to 350° F as quickly as possible. The samples were held at 350° F for ten (10) hours before they were

removed from the furnace. Once removed, they were allowed to cool at room temperature (no quench).

2.3 Testing

A rigorous testing regime is crucial to understanding the metallurgical properties of the welded component and determining the feasibility of the additive friction stir welding process. The most critical properties of most components that could be manufactured using AFSW are the tensile strength and elongation. The most direct method for measuring the tensile strength and elongation are through uniaxial tensile testing. In addition to tensile testing, non-destructive testing was performed to directly evaluate the difference in samples before and after heat treatment. Previous work has been done including tensile test and macrographic photos through the NCAM class project for Al 2195-T84, but no similar work has been done with Al 2219-T87

After samples were welded as discussed in section 2.1, followed by cutting and machining to bulk sample, they were subjected to a battery of test to determine the mechanical properties both before and after heat treatment. The machining included removing the unwelded and the hole left in the surface from the pin removal during the welding process with band saw. Remaining block included the dwell, the weld stack, and the unwelded sections on each side of the weld stack. The surface of the final weld was fly cut to remove welding tracks along the surface of sample and create a smooth surface. The retreating side of the weld stack was machined down to the weld nugget by fly cutting and the dwell portion of the stack was removed using a tile saw with water as coolant to reduce the surface temperature during cutting. Both the start and the end of the weld, which were cut away from the bulk sample, were saved to be polished.

2.3.1 Rockwell Hardness

To evaluate the mechanical properties before and after heat treatments, non-destructive testing was used. It has been shown in several materials that there is a direct correlation between hardness and strength [15, 16, 17]. The correlation will not be as accurate as direct measurements of either the 0.2% offset yield strength (YTS) or the ultimate tensile strength (UTS). Since direct measurements of strength were also measured for this thesis, Rockwell hardness (scale B) was used to determine relative changes in the strength through the entire process. It can be used to compare the change in parent material to the welded sample both before and after heat treatment.

Rockwell hardness testing was performed in accordance with ASTM procedure [18] along the surface of the final weld. Before heat treatment, the bulk sample was tested along the length of the final weld to determine the initial Rockwell hardness. Due to the expected material properties, the samples were tested using the Rockwell B scale and procedure, which included the use of a 1/16-inch diameter carbide ball indenter along with a 10 kg (22.05 pound) minor force and a 100 kg (220.5 pound) major force with a 2 second dwell time. ASTM procedure requires a minimum spacing of three times the diameter of the indenter from center to center of the testing indentions to reduce the effect of one measurement on the next.

Rockwell hardness was measured along the center line of the weld both before and after heat treatment. To maintain the required minimum spacing before and after the heat treatment and still maintain a valid measurement over the length of weld, the preheat treatment measurements were taken at 3/8-inch increments. The post heat treatment measurements were taken at alternating intervals to maintain the overall spacing of 3/16-inch center to center. To determine a parent material hardness, additional hardness measurements were taken on virgin, unwelded Al 2195 and Al 2219. The results of the Rockwell hardness tests are presented in Chapter 3.

2.3.2 Sample Polishing and Macroscopy

In addition to Rockwell hardness, the start and end cutoffs were characterized through macrographic photography, micrographic photography, and Vicker's microhardness testing. Before testing could be performed samples were polished and etched to show the crystallographic grain structure along with any defects and artifacts formed through the welding process. The samples to be polished were left essential intact to show the profile of the entire weld stack. Due to the specimen size, all samples were polished by hand.

Since the samples to be polished were initially rough cut using a band saw and tile saw, it was important to develop a flat working surface that would show a direct cross section of the weld, although care had to be taken not to damage the surface at the same time. All polishing was done using a Struers Tegrapol-1 Polishing machine, which has a variable rate of speed and an automatic water feed. Any significant sample shaping was done by using 80 grit sand paper with the turn table at approximately 100 rpm. Great care had to be taken both to hold the sample in position and to prevent damage to the sample surface caused by the course grit sanding paper. The next step in the polishing process included 220 grit sand paper, which was used primarily to remove any large gouges from the grinding process and to establish a flat surface. Once the 220 grit step in complete based on a visual inspection, 320 grit sand paper was used at 80 RPM for approximately 3 minutes. The 320 grit was followed by 500 grit again at 80 RMP for approximately 1 minute. Once a consistent surface has been achieved using 500 grit paper, 2400 grit paper was used at 100 RPM. Next, the Mol polishing pad is used in combination with a 3μm diamond lubricating suspension. The final step incorporates a Chem polishing pad using an OP colloidal silica oxide suspension. It is important to note that after each step the sample was inspected for any larger than average scratches or gouges in the surface. If there were any inconsistencies in the surface the polishing

process was taken back to the previous step (or two if the gouges were significant) to ensure a consistent surface.

Once the samples have been thoroughly polished, the samples were etched using a diluted Krolls etchant, which is a solution of distilled water, nitric acid, and hydrofluoric acid, used to bring out the metallic grain structure of the surface of the sample. Due to the strength of the Krolls etchant solution, the surface etched exceedingly quickly (within a few seconds) if a full-strength solution was used. To solve this issue, a dilute etchant solution was used in conjunction with a basic solution consisting of baking soda and distilled water to use as a stop bath once the etching is complete. Upon completion, the samples were allowed to run under water for several minutes to ensure the surface no longer contains any acidic solution. For safety reason, the etchant solution was disposed of with care by adding the small amount of etchant to the larger basic stop bath. The pH was measured using a universal indicator solution to ensure that it was safe for disposal. Once the surface has been polished and etched, high resolution photos using a macrographic lens were taken to visually characterize and inspect the weld cross section.

2.3.3 Metallography and Vickers Microhardness.

The friction stir welding process described in Chapter 1 can significantly affect the metallographic grain structure and thusly mechanical properties throughout the weld area. The initial strength of the parent material is often dependent upon the way the material was fabricated. Manufacturing techniques are often used to prestress the material, including working and heat treating the materials to refine the grain structure and increase strength. Friction stir welding uses a combination of the forge and rotational forces will plasticize the aluminum as the pin tool translates along the weld. Once the material has been brought past the elastic limit and plasticized, the work within the weld nugget is removed and the initial grain structure is significantly changed,

generally a very fined grained structure. The shoulder will reforge the material and can impart some work into the weld nugget. Away from the weld nugget, a combination of forge force and heat will create thermos-mechanical zone that will have an increase in strength due to the work input and the heat from the welding. This process is similar to hot rolling. Further from the weld the material is heated through the welding process, but does not experience the work associated with thermos-mechanical zone. This area is essentially annealed, which in most materials will reduce the strength compared to the parent material.

Since the mechanical properties vary throughout the weld, it is important to characterize the grain structure to understand the mechanical properties throughout the weld. Macrographic photography can be used to visually inspect the differences, but this does not allow for a quantitative analysis of the weld. Both metallography and microhardness measurements can be used to help analyze the samples.

Metallography is the study of the microstructure of metals and metallic alloys through a variety of techniques. It includes the determination of constituent materials of samples and structural and special distribution of the metallic alloys. Although metallography can incorporate a variety of techniques to achieve its goal, it most often includes the use of incident light microscopy on highly polished and etched samples to view and characterize the sample surface. Although incident light microscopy is the most common techniques a variety of other methods including tinted etchants, darkfield microscopy and differential interference contrast microscopy to add additional contrast. The described methods used in conjunction a calibrated microscope can be used to determine the presence of and analyze surface defects and measure the grain size at the surface of metallic samples. It is important to understand that these techniques are two-dimensional methods and does not account for anisotropic grains. Even though metallographic microscopy has

the capacity to quantify the grain size, this thesis incorporated it to determine the relative variations in grain size throughout the polished samples especially at the weld zone boundaries.

Although understanding and measuring the variations in grain sizes across a sample using metallography techniques can be helpful in understanding the mechanical properties, comprehending the failure of a sample, and providing some quantitative analysis, microhardness testing can be used to determine relative changes in strength of a material, both throughout the surface and as the sample undergoes various processes. Similar to Rockwell hardness testing, microhardness testing uses an indention device with a specific load to determine the material resistance to penetration. Again, as with Rockwell hardness, this resistance can be used to determine the relative mechanical properties. Rockwell hardness is used to determine the bulk hardness of a large sample, while microhardness can be used on a smaller scale to determine variations of hardness. Microhardness uses a ratio of the applied force and the cross-section area (at the surface) of the indention to determine the local hardness.

Microhardness testing uses a calibrated pyramidal diamond indenter, which typically comes in two shapes. Knoop testing utilizes an asymmetrical pyramidal indenter with a 7:1 length to width ratio, while Vickers hardness uses a symmetrical pyramid. Minor variations between the measurement techniques exist, and some evidence has shown that Knoop hardness testing produces lower hardness values than Vickers hardness tests for higher hardness materials and lower values than Vickers for lower hardness materials [19]. This difference is not considered significant.

Since Vickers hardness uses a symmetrical pyramidal indenter, the surface area of the indention is determined by taking the average of the two diagonals of the resultant diamond. Based

up the geometry of the pyramid, the surface area of the indention is determined according to the formula,

$$A = \frac{d^2}{2\sin(136°/2)} \approx \frac{d^2}{1.8544}, \quad 2.3.3.1$$

The Vickers microhardness (HV) is determined by the ratio of the applied force over the indention area

$$HV = \frac{F}{A} = \frac{1.8544\,F}{d^2}, \quad 2.3.3.2$$

To accurately determine the microhardness, one must choose the appropriate applied force for a given material. To determine the appropriate applied force, the HV is measured using a variety of forces. Graphing the measured hardness versus the applied force shows that a minimum applied force is required to overcome the elastic properties of the material as seen in figure 15. Once the minimum is determined, the applied force that creates the appropriate size intention is the one that should be chosen. In general, the indentions are approximately 50 μm, which requires a microscope to measure the surface area. Manual testing uses an optical scale attached to the viewing lens that can be rotated to measure the desired diagonal, in conjunction with manual sample stage which uses micrometers to carefully move the sample along both the x and y axis. More modern testing machines are able to use a computer controlled automated sample stage with a digital camera. The modern setup can be used take single measurements or allows for a preprogrammed measurement patterns. The specialized computer programs associated with the automated system can digitally measure the surface of the indentions, but this is not always accurate and often measurements must be verified and/or reevaluated.

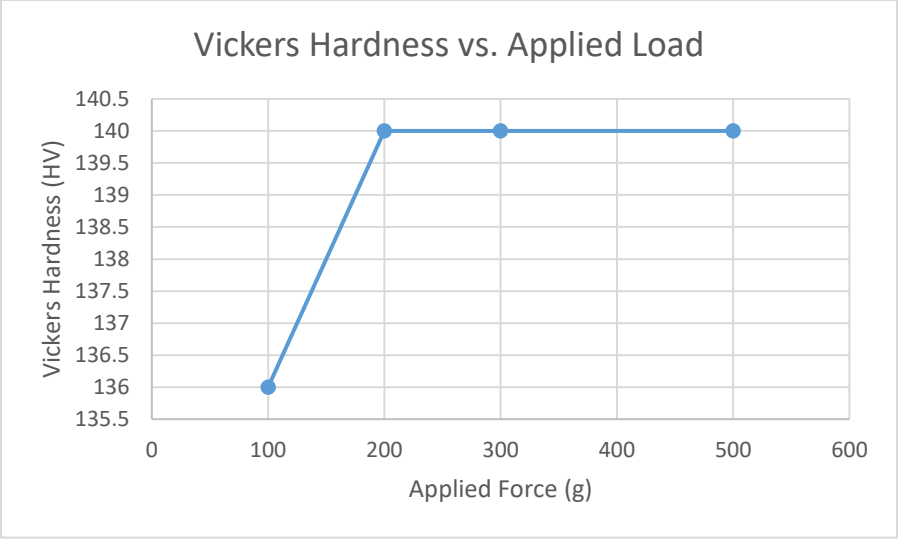

Figure 15 Graph of the Vickers microhardness (HV) vs. the applied force (grams) is used to determine the appropriate load for further measurements.

To measure the microhardness of the polished samples, Vickers microhardness testing was performed using a Newage HMV-2 Microhardness tester. Although the HMV-2 tester has the capacity for digital measurements, all testing was done in the manual mode. Based on the results of applied load testing as shown in Figure 15, an applied load of 200 g (1.961 N) was used since it both overcame the elastic properties of material and produced the appropriate sized indention. A limited testing regimen was developed with the goal of both characterization of individual weld properties and for comparison between welds within a sample and between samples., before and after heat treatment. The testing program included characterizing three (3) welds, weld 3, weld 8, and weld 12, on each of the polished samples. The welds were characterized by three (3) evenly spaced (2.5 mm apart) horizontal lines as shown in Figure 16. Each line consisted of evenly spaced individual measurements (0.5 mm) across the entire sample to evaluate the cross-section.

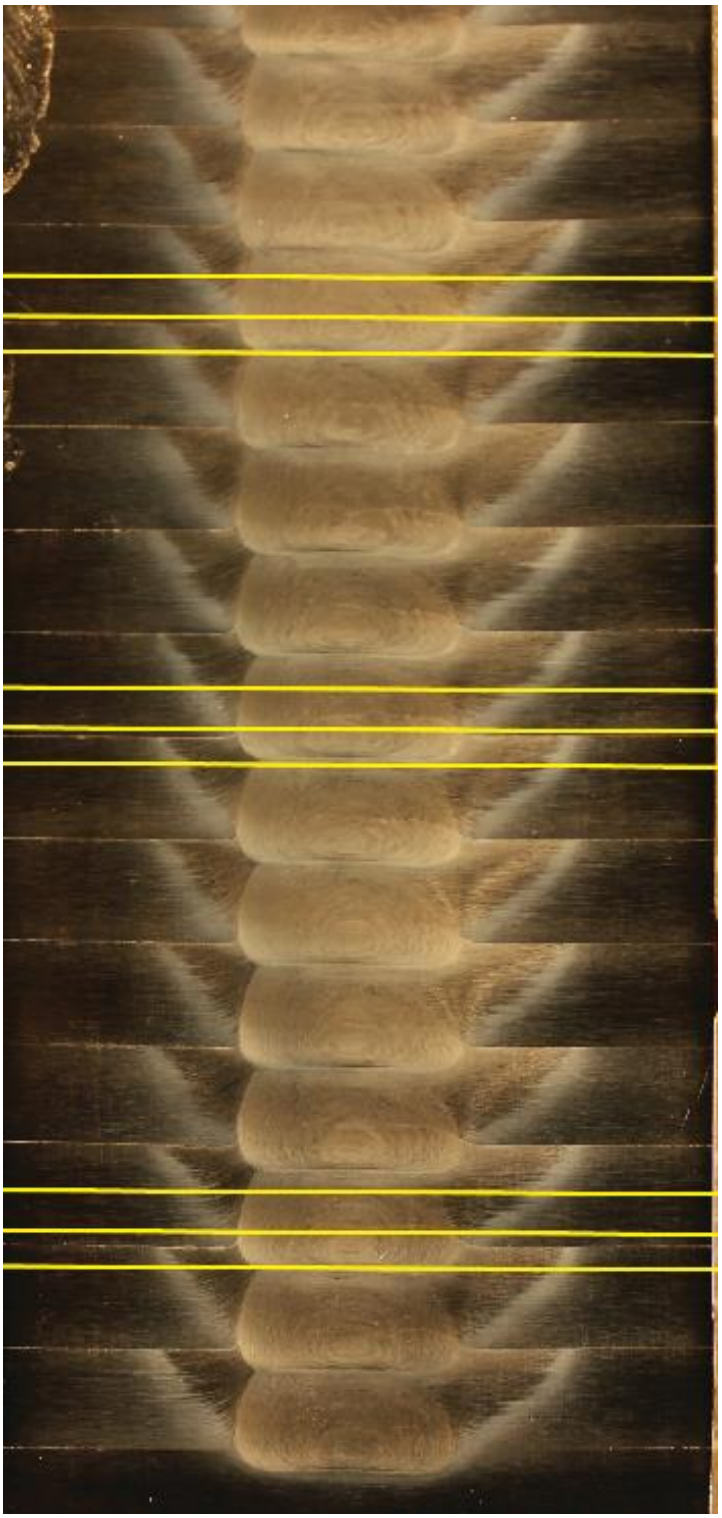

Figure 16: Three welds on each polished sample were characterized using Vickers microhardness testing. The cross-section of the individual welds was evaluated by measuring the microhardness across three evenly spaced horizontal lines: across the root, through the center, and near the top of the weld. Each line consisted of individual measurements taken at 0.5 mm increments.

It is important to note that Vickers hardness testing is generally performed according to ASTM E92-16 [20]. The standard method involves taking the average over several measurements in a grid like pattern to determine the HV value in a localized area. The purpose of this thesis was to determine a hardness profile of the cross-section, which was performed outside the scope that ASTM standard. All spacing standards were met to minimize the effect individual measurements on each other.

2.3.4 Tensile Testing

Although the non-destructive described in sections 2.3.1 through 2.3.3 testing can provide a great deal of indirect information, destructive tests such as tensile testing can determine several mechanical properties that lead to a direct understanding of a material. Tensile testing is used develop a stress versus strain curve that characterizes the resistance of the coupon to breaking under tension. The curve is developed utilizing a load frame that is capable of pulling a sample at a controlled linear rate in conjunction with a load cell that measures the force required to pull that sample. The load frame used for testing in this thesis was the MTS 810 Uni-Axial Universal Test System. Strain plotted in the curve defined as the change in length of a sample divided by the original length as shown in Figure 17. During tensile testing, the strain is the independent variable produced by pulling the sample apart at a constant linear rate. The stress is the dependent variable calculated by the dividing the force resulting from the applied stress, as measured by the load cell, divided by the cross-sectional area of sample. An important distinction should be made here regarding the cross-sectional area. As the sample is subject to strain the sample will elongate, reducing the cross-sectional area. If this changing cross-sectional area is used in calculations, the stress is known as true stress. The true stress is particularly difficult to determine since the cross-section changes during testing. Due to this difficulty, stress versus strain graphs use the initial

cross-sectional area to calculate the stress throughout the entire testing process, which known as engineering stress.

$$Strain = \varepsilon = \frac{\Delta L}{L}, \quad 2.3.4.1$$

$$Stress = \sigma = \frac{F}{A} \quad 2.3.4.2$$

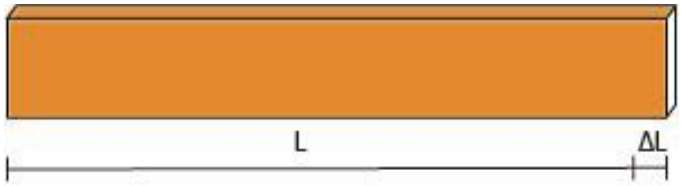

Figure 17: Strain is defined as the change in length (ΔL) of a sample divided by the original length (L)

Although the final output of a tensile test is a stress versus strain curve, the tester does not measure these values directly. The universal test system is an incredibly powerful, yet simple machine. It consists of a load frame with a crossbar, which can be adjusted using the hydraulic pump. Before any testing occurs, the crossbar is clamped into place and used as a fixed position throughout the test. Attached crossbar is load cell along with a hydraulic grip. Opposite the fixed position crossbar, another hydraulic grip is attached to a hydraulic piston. The position of the piston is carefully measured throughout the entire testing process. The tensile test is run by placing a sample into the machine between the grips and pulling the sample apart at a designated rate. As the sample is pulled the position of the piston is recorded along with the force required to pull the sample. The stress is calculated according to formula 2.3.4.1, where the cross-sectional area is measured before testing. Strain is measured in one of two ways though. If a necked town sample is used, the initial length is given by gauge length determined before testing begins and the change in length is difference the distance the piston has moved at the time of measurement. Although this method seems direct, it does not account for the fact that the machine itself and its components

will flex under a load. This can be accounted for by running a machine deflection test to determine the amount the flex for a given load. The flex is calculated by running a sample that will not elongate under a large load (i.e. a thick block of steel) with essentially no distance between the grips. The slope of the resultant force versus deformation curve, which should be essentially linear, is used to account for any machine deflection in the strain calculation. A more direct measurement technique uses an extensometer directly attached to the necked down section of the coupon. The extensometer has a precise initial distance and will directly measure the change in length. The use of an extensometer greatly reduces the uncertainty associated with both the machine deflection and the movement of the piston, while accurately and directly measuring the strain.

Before any testing was performed, the samples are carefully prepared according to ASTM E8/E8M-16a for a 0.25-inch sample thickness [21]. Once initial machining is done to obtain raw coupons, the samples are fly cut to a width of 0.375 inches. The final step in sample preparation is using an end mill to create a necked down section of the coupon creating a dog bone shape. The necked down section creates a 0.25-inch by 0.25-inch square cross section. A diagram showing the measurements for the coupons can be found in Figure 18. Due to the smaller cross-sectional area, most of the coupon's elongation and failure will occur within the necked down portion.

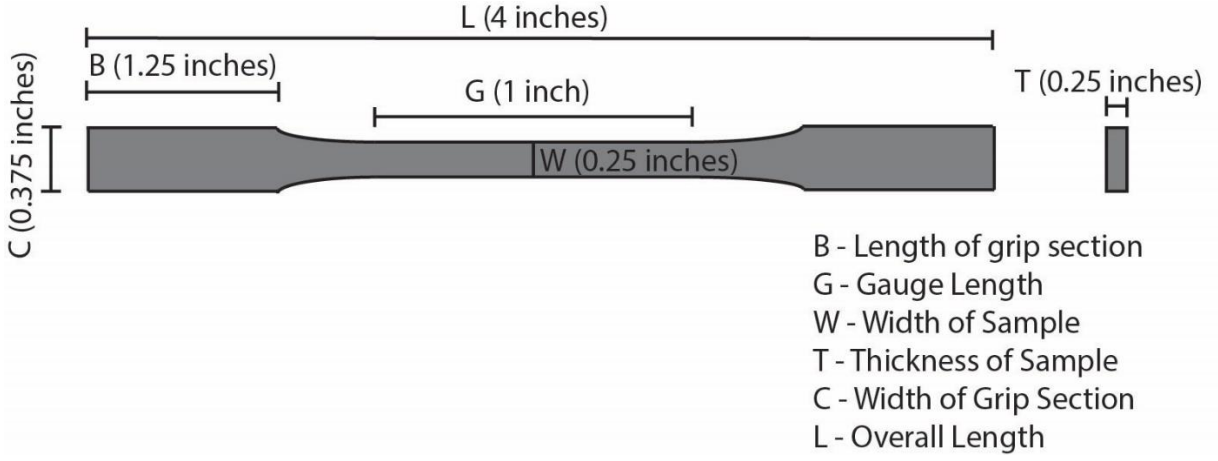

Figure 18: The ASTM standard for manufacturing 0.25 thick tensile samples

The resultant stress strain curve can provide great understanding about the strength of the tested sample. The graph itself is used to calculate both the 0.2% offset yield and ultimate tensile strength. As seen in the graph in Figure 19 the curve has two distinct regions. The initial linear portion of the graph is known as the elastic region. This region is particularly important to characterize because it describes the amount of stress a material can tolerate before becoming permanently deformed. In addition, the Young's Modulus is defined as the slope of this linear portion. The maximum stress in the elastic region is known as the yield strength, which is determine by calculating the slope of the elastic region (the Young's Modulus). The resultant line is offset by 0.2% strain. The point at which this line intersects the stress versus strain curve is known as the 0.2% offset yield strength.

Beyond the yield strength, the slope of the curve abruptly changes and is generally reduced. The area between the yield strength and the final failure defines the plastic region. A sample that has been placed under enough stress to be plasticized will remain deformed when the stress has been removed. Additionally, the ultimate tensile strength, which is the maximum stress that the material can experience before failure, is easily found based on information contained within the stress-strain curve.

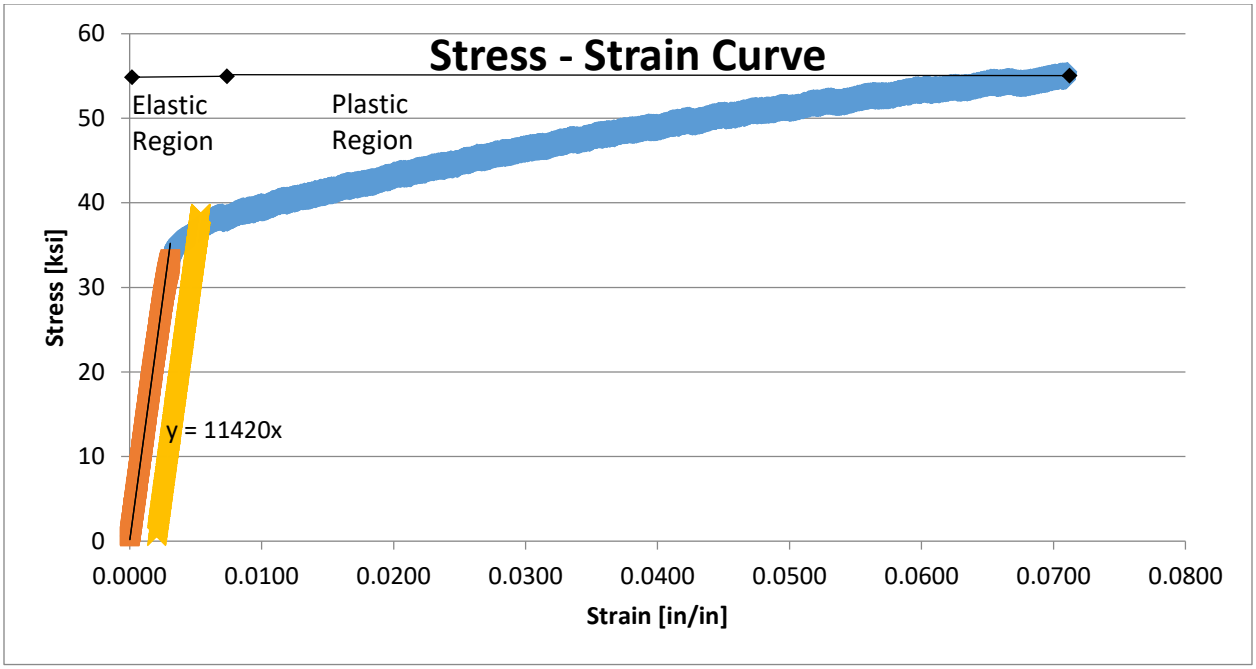

Figure 19: The representative Stress vs. Strain curve

In addition to the properties described above, one can also use tensile testing to determine the ductility or the percent elongation. Ductility is used to describe the ability of a material deform under stress. It is defined as the change in the gauge length after fracture divided by the original gauge length expressed as a percent. This change can be measured using an extensometer, or using gauge marks a fixed distance apart. If neither are used the distance between the grips is used as the gauge length. In the tensile samples for this thesis, the available extensometer was not suitable for elongation measurements. Gauge marks were imprinted outside the necked down section of the coupons. The initial measurements were verified before tensile testing. Upon completion of the test, the sample was put back together and the distance between the gauge was measured again. The percent elongation was then determined as described above.

Chapter 3: Results and Discussion

3.1 Macroscopic Photography

After sample polishing extensive macroscopic photos were taken both before and after post weld heat treatment. Comparing photographs of the same weld within the stack at the dwell location and the pin removal helps to develop a profile along the translational length of the weld. In addition, using photographs taken after heat treatment, it is possible to determine any major changes in the sample due to the treatment.

Figure 20 shows, the weld profile for 2195-T84 is relatively consistent along the length of the sample. The photographs taken near the start of the weld show that it may not be fully developed at the location that the sample was removed from the bulk. Due to the use of the flared pin tool the weld nugget maintains a similar shape. Each of the welds experiences hooking on the advancing side and sheet thinning that extended approximately half way into the weld nugget. It is important to note that these are features commonly associated with lap welds and are not considered defects. They do not necessarily affect overall strength of the samples. Additionally, some small voids along with localized areas of lack of consolidation were observed within the weld nugget. These are generally caused by excessive rotational speeds or a lack of forge force. Figure 21 depicts the results of heat treatment. Based on the macrographic photos, only nominal differences exist. These samples had to be polished again after treatment, which can be attributed to the repolishing process that was performed post heat treatment.

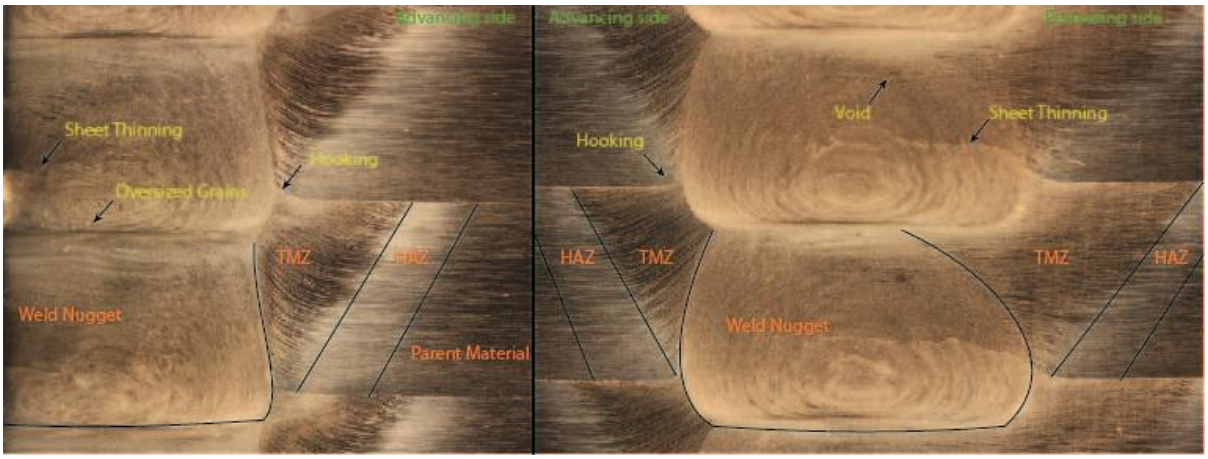

Figure 20: The representative images taken of the eight weld of both the start and end polished sample of as welded 2195-T84

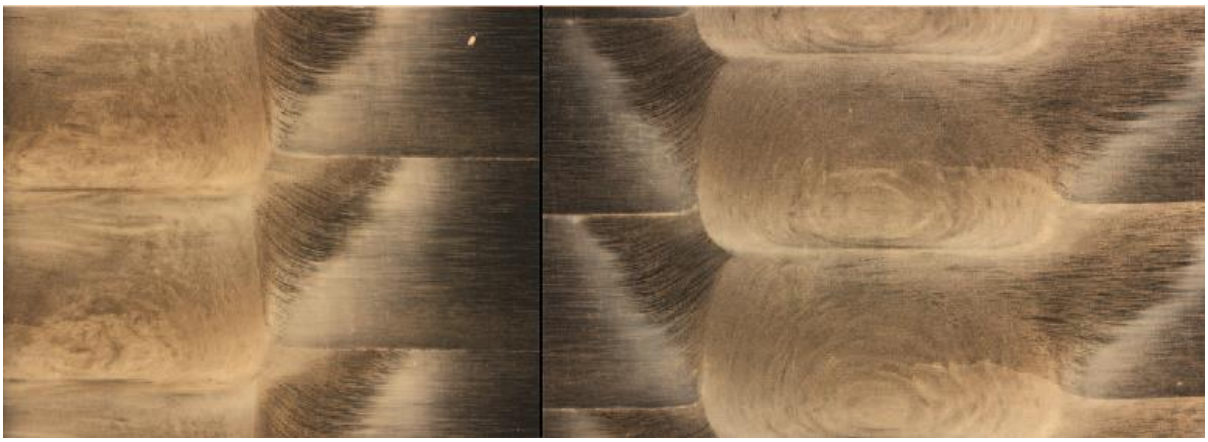

Figure 21: The representative images taken of the eight weld of both the start and end polished sample of post heat treatment 2195-T84

The photographs of the 2219-T87 as seen in Figures 22 and 23 show a very difference cross-section. Even though the welds were performed with the same pin tool, the profile of the weld nugget was squarer than the 2195-T84. The shape of the weld nugget indicates that the tool was better able to stir the 2219-T87 compared to the 2195-T84. Another key difference the size of the thermo-mechanical zone (TMZ) and the heat affected zone (HAZ). This could be due to the properties of the base 2195-T84 that require a much higher heat input was required to plasticize the material. The additional hear required to plasticize the 2195 creates a larger HAZ.

It is very important to note several unexpected issues in the welding process. It was noticed in both materials that after approximately four stacked welds, the pin tool would begin to dive further into the surface than the initial welds creating extra flashing and significant welding tracks. This was somewhat controlled by manually increasing the translation speed during the weld once the tool started to sink. The problem was much more difficult to control in the 2219-T87. Even though the welded surface was sanded, the tool dug too far into the sample in these later welds to create a flat working surface. This did not seem to affect the weld nugget, which was the area of most interest, but visible gaps can be seen at the end of the weld as shown in Figure 22 and Figure 23.

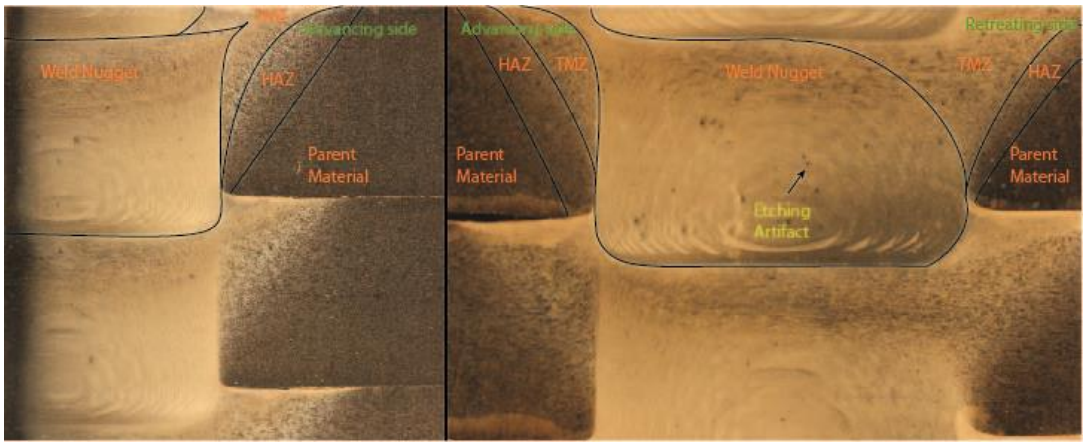

Figure 22: The representative images taken of the eight weld of both the start and end polished sample of as welded 2219-T87

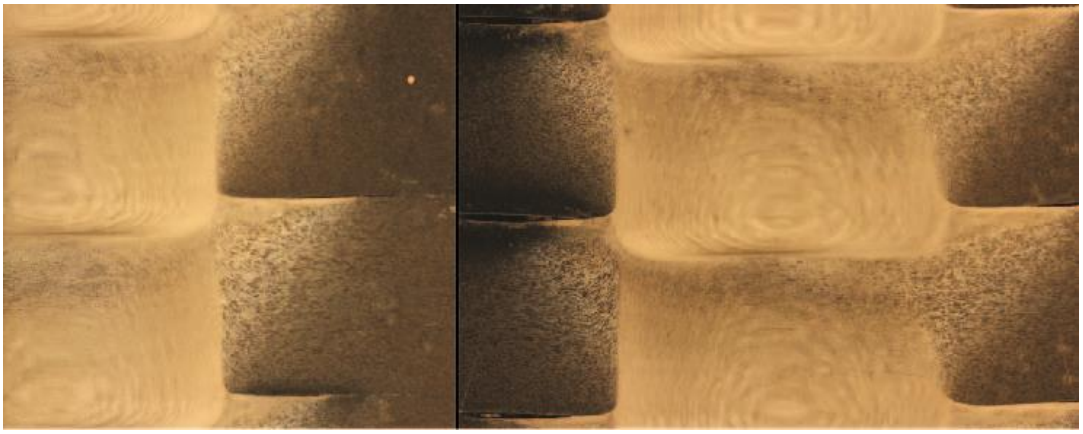

Figure 23: The representative images taken of the eight weld of both the start and end polished sample of post weld heat treated 2219-T87

3.2 Rockwell Hardness

As discussed in Chapter 2, Rockwell hardness was measured along the surface of the final weld according to ASTM standards. All measurements were taken using the Rockwell B scale, which utilizes 1/16 inch diameter tungsten carbide ball, a minor force of 10 kgf, a major force of 100 kgf, and a 2 second dwell time. Although ASTM standards require a minimum spacing of three (3) times the diameter of the indenter, initial testing was performed at six (6) times the diameter. This was done so that measurements could be taken along the entire length of the weld both before and after heat treatment. The reported Rockwell Hardness B (HRB) values were determined by calculating the average over twelve (12) individual measurements. The results of are presented in Table 1.

Table 1: Rockwell B Hardness Results

Initial Material	Parent Material (HRB)	Pre Heat Treatment (HRB)	Post Heat Treatment (HRB)
2195-T84	77 ± 2	62 ± 2	66 ± 1
2219-T87	72 ± 2	46 ± 2	68 ± 2

It is no surprise that the HRB of the welded samples is less than that of the parent material. The 2195 weld prior to heat treatment was approximately 81% the value of the parent material and 86% after, a 5% increase. While the as-welded 2219 was only 64% the value of the parent material, after heat treatment the hardness increased to 94% the value of the parent material, an increase of 30%. Based on the results of the hardness testing, the as-welded 2195-T84 maintains a reasonable hardness and only increased minimally based after heat treatment. In contrast, the welded 2219-T87 had a significant reduction in hardness, but when heated treated increased significantly to nearly the value of the parent material. It is important to take into consideration that the hardness was only measured on the surface of the final weld, and the above results may not be indicative of

the entire sample. Additionally, tests were not performed immediately after welding. Some undocumented natural aging may have had some minor effects on the results.

3.3 Metallography and Vickers Microhardness

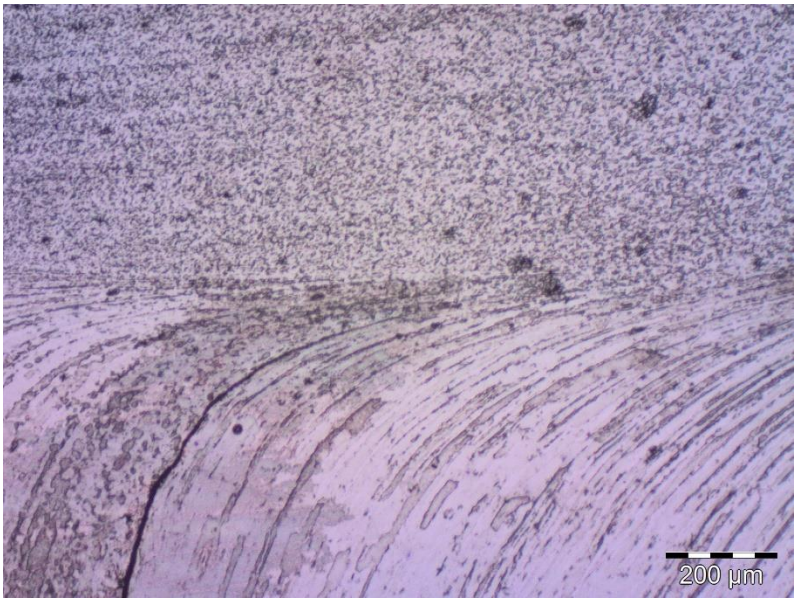

Figure 24: Metallographic techniques were used to photograph the point at which two plates meet and are stirred into the weld nugget becoming a single component. This picture was taken on the advancing side of the third weld in the 2195 component.

The metallographic testing included taking micrographic photographs in areas of interest such as the interface between weld zones and areas of potential defects. The stark differences in grain sizes between some of the weld zones can be seen in Figure 24. The four images in Figure 25 below help provide insight into the effect of welding on the material. The focus of this thesis is to generally determine the feasibility of creating a component, with minimal machining, made entirely of the weld nugget. To that end, microscopy was used to evaluate and understand potential areas of failure. It should be noted that metallography generally can be used to measure the grain sizes of a sample, but no measurements were taken here due to the significant variations even in localized areas of the sample as shown below in Figure 25.

Figure 25 shows some of the more important areas of the weld nugget, the most important being the is intersection of the two lap welds. The upper left image in Figure 25 shows this intersection. The left side of the micrograph is the top of the second weld in the stack, while the right side shows the bottom of the third weld. The white line in the center of the photograph is the boundary between individual welds. The first thing to notice about the image is the small voids throughout the photograph. These voids may affect the overall strength of the sample and possibly indicates a lack of consolidation. The second feature to notice in the picture is the significant variation in grain size over a small area. The upper weld to appears contain relatively consistent equiaxed grains, but the lower weld has grains that vary in both size and shape. These anisotropic grains along with the clearly defined boundary between the welds potentially creates an area of lower strength within the weld stack and likely location at which the sample will fail.

The second image depicts the typical view of the apparent fine equiaxed grain structure found within the weld nugget. The grain size and shape vary throughout the photographed area. Even with the differences in size, the grains are small enough that the variations will not affect the overall strength of the material. It can also be seen that precipitates have form at the grain boundaries increasing the strength of the as welded sample. The final two photographs are close-up images of the sheet thinning weld artifact that was discussed previously. Even though the image was taken at 50 X magnification, the sheet thinning artifact still appears to be a crack or scratch. By increasing the magnification to 200 X, it can be seen that the sheet thinning artifact is not a continuous line but actually appears to be a series of disjunct areas of excessive precipitation or residual oxidation on the sample surface. All photographs in Figure 25 were of the 2195 in the as welded condition. Additional images of were taken of 2219 and 2195 in the as welded and post

heat treatment state, but no notable differences were seen the images. The images in Figure 25 are representative of common features found in all the welds.

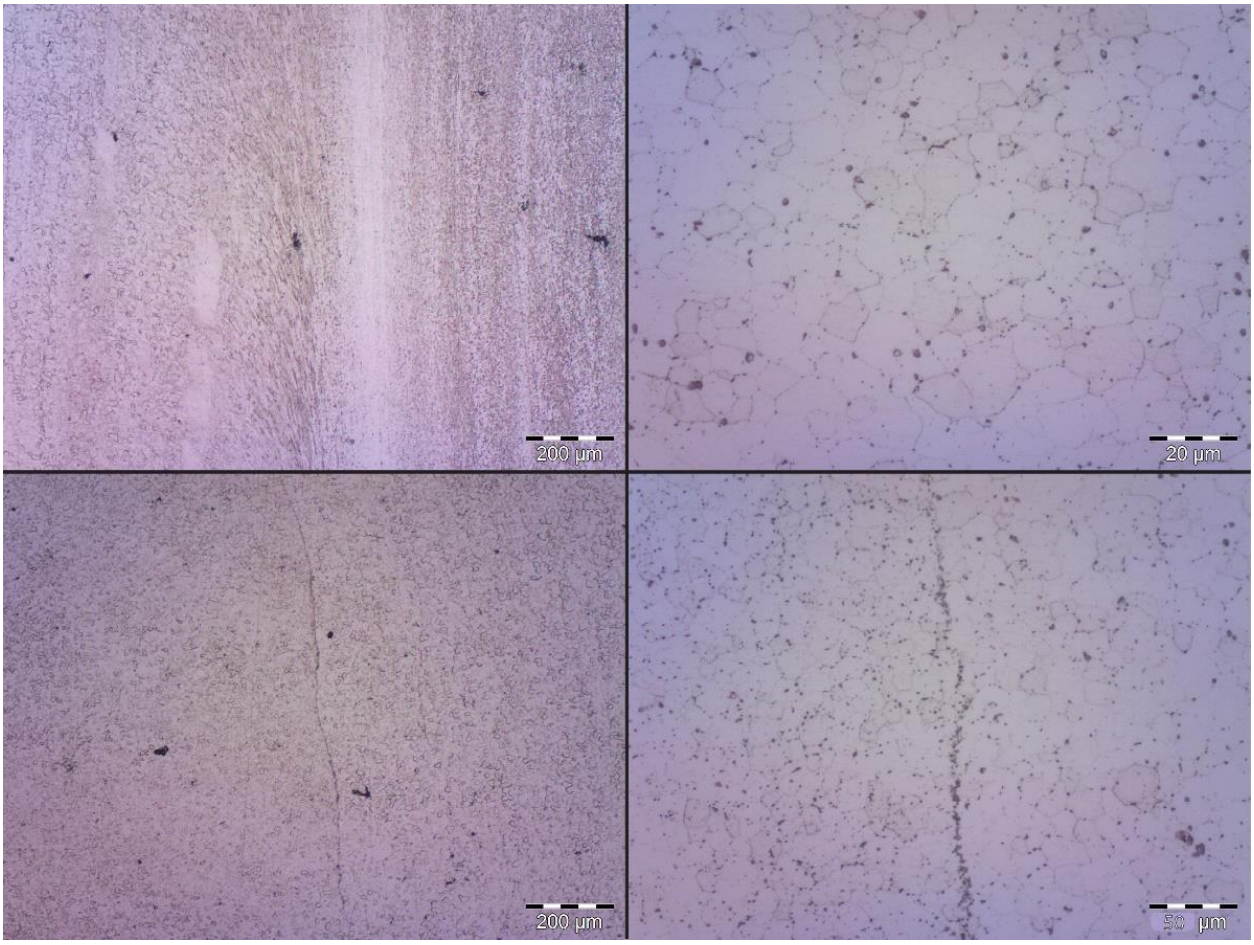

Figure 25: The top left) image shows the variation grain size at the interface between welds. The top right) photograph is a close-up image taken within the weld nugget at maximum magnification. At this magnification it is possible to distinguish the grain boundaries along with the precipitate growth at the grain boundaries. The bottom left) image depicts the sheet thinning encountered in the weld. The bottom right) image is a zoomed in photograph of the same sheet thinning.

In addition to using metallography techniques to characterize the weld nugget, the results of the microhardness testing regiment, as discussed in Chapter 2, allows for comparison of the metalographic properties measured within individual welds, welds in a single sample, and between materials, both before and after heat treatment. Due to the volume of microhardness data collected,

it is not feasible to discuss all the results in depth here. For the purpose of analysis, weld 8 of the two end samples has been treated as a characteristic weld, as it was in sections 3.1.

Even though measurements were taken across the entirety of the weld, evaluating the effect of the heat treatment within the weld nugget is the primary goal of this project and will help determine the ultimate effect of treatment on a manufactured component. The vertical lines in Figure 26 and Figure 27 represent the approximate width of any final components manufactured using this method additive friction stir welding.

Reviewing the results as depicted in Figure 26 shows that in 2195-T84 the Vickers hardness along the bottom and middle of the weld was not meaningfully affected by the heat treatment. Some increase in the top portion of the weld was observed though. As somewhat expected, the minimum hardness values were measured at the boundary between the welds. The hardness values measured in the 2219-T87 sample (Figure 27) showed remarkable consistency throughout the weld nugget prior to heat treatment. The middle of the weld showed moderate increases in the Vickers hardness, but it was not consistent across the weld nugget. The most noted increase in the hardness was observed at the top of the weld nugget. With an initial average value 90±1HV within the weld nugget and a final average value of 119±1 HV, the top of the weld was observed to have an increase in hardness of approximately 32%. This is similar to the increase that was observed in the Rockwell testing of the 2219-T84.

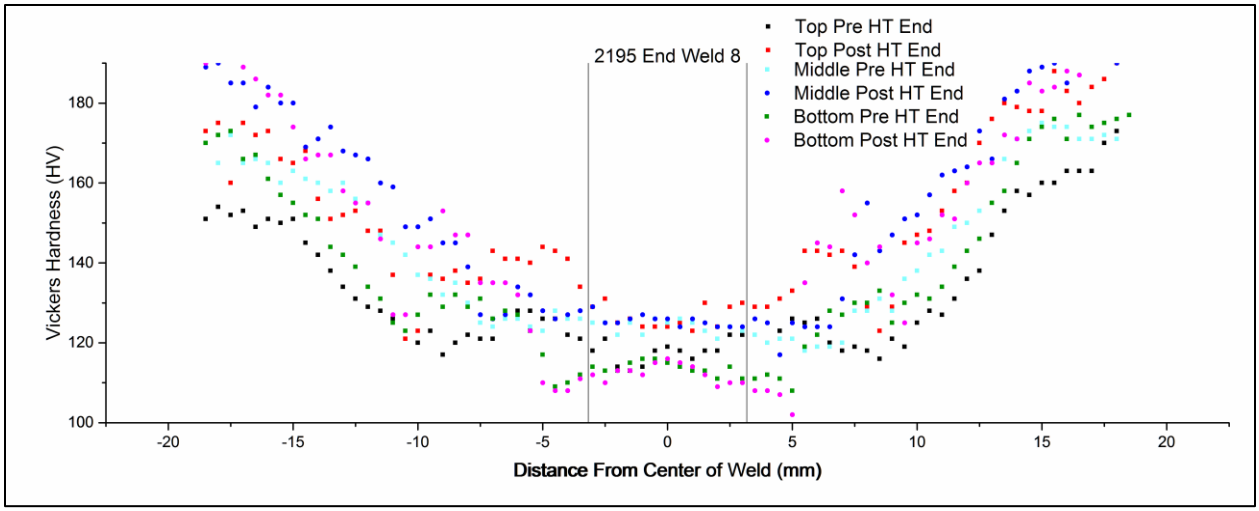

Figure 26: Microhardness values were measured as discussed in Chapter 2 both before and after heat treatment. The results were graphed as the Vickers hardness values (HV) vs the distance from the center of the weld (mm). The graph depicts all the microhardness measurements performed on weld 8 of the 2195 end sample. The vertical lines near the center represent the width of the tensile coupons.

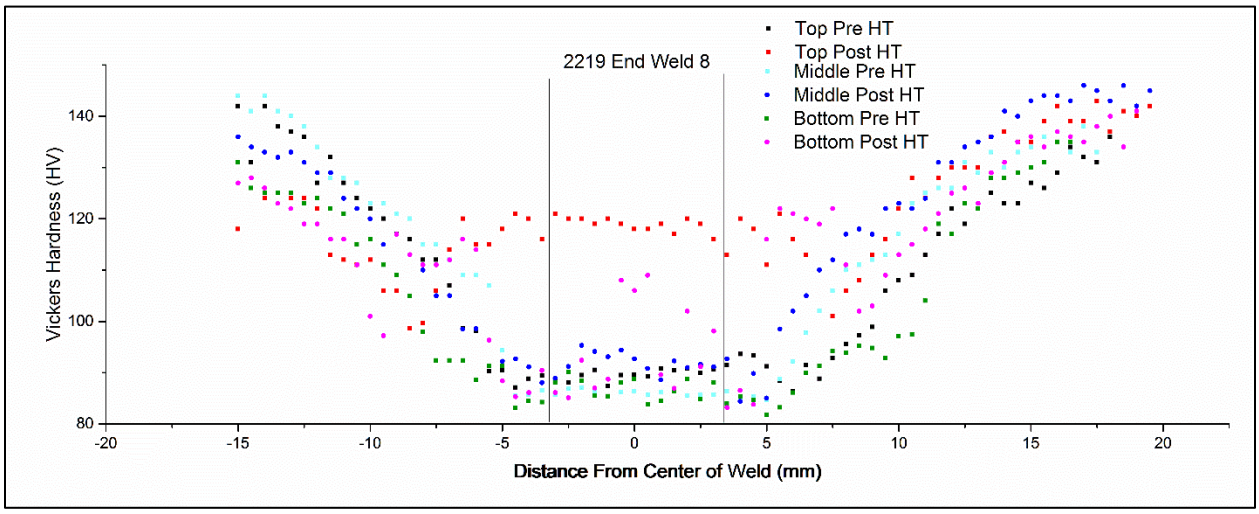

Figure 27: A comparison of the of all the microhardness measurements in weld in 8 of the end sample shows a largely consistent microhardness in most areas. The values measured in the top of the weld showed significant increase after heat treatment.

3.4 Tensile Testing

The tensile strength tests were performed to attain the ultimate goal of understanding the welded material and its capacity for use in manufacturing. Since the yield strength and ultimate strength values are often used in the design process. The values shown in Table 2 are the

established properties of the base material. All the welds performed for this thesis were performed through the short transverse (ST) and the final coupons were pulled in the ST grain direction. A quick glance at the 2195-T84 has higher strength values than 2219-T87, 33% high yield tensile strength and 34% higher ultimate tensile strength, making it a preferable choice for welding at first glance. This does not necessarily mean that 2195-84 will be compatible with the friction stir welding process or heat treatments. It should be noted that the base elongation data is not available in the ST grain direction for either 2195-T84 or 2219-T87.

Table 2: Base 2195-T84 and 2219-T87 Material Properties [13, 41]

Material	YTS (ksi)	UTS (ksi)	Elongation %
2195-T84 ST 2" Coupon	65	71	N/A
2219-T87 ST 4" Coupon	49	53	N/A

The NCAM FSW class fabricated two multiple lap weld stacks, one using a straight pin tool and the other using the flared pin tool. The samples were machined as described in Chapter 2 and tensile testing was performed. The results of the as welded flared pin tool tensile tests are presented in Table 3. On average, the yield strength (ksi) was found to be about 55 % that of the parent material and the ultimate tensile strength (ksi) is approximately 75% that of the parent material. The reduction in strength is to be expected since the welding process generally removes any work in the parent material, even though some work is put back into the system as the shoulder reforges the material.

These results provided a good basis for understand the effect of the baseline heat treatment on the material strength. The results of the tensile testing on the heat treated 2195-T84 are presented in Table 4. Taking the average over all the tested heat treated 2195-T84 samples shows that the yield strength after heat treatment is approximately was about 57% that of the parent

material. In addition, the ultimate tensile strength was about 59% that of the parent material with an average elongation of 3.5%. In comparison to the samples that did not undergo any heat treatment, the YTS increased nominally (about 2%) and the UTS was reduced to 59 % that of the original material, a reduction of 16%. Based on the stress strain curves of both the as welded and the post heat treated (Figure 28) 2195-T84, it appears that the post heat treated samples failed shortly after reaching the YTS. Based on the current information, the nature of the reduction in UTS cannot be determined. It is most likely that the heat treatment reduced the ductility of the coupons causing the samples to reach UTS much faster. The early fracture may also have occurred due to a single poor-quality weld within the stack or damage to the samples during the machining process. Further investigation will be required to determine why the heat treated samples had such a reduction in UTS.

Table 3: NCAM FSW Class Flared Pin Tensile Results 2195-T84

2195-T84 (No Heat Treatment)	YTS(ksi)	UTS(ksi)	% Parent Material YTS	% Parent Material UTS
FF1	36.9	55.5	57	78
FF2	33.6	49.3	52	70
FF3	37.8	55.9	58	79
FS1	35.8	48.6	55	68
FS2	36.6	54.5	56	88
FS3	35.3	48.7	54	69
Average:	36	52.1	55	75

Table 4: Calculated Results of Heat Treated 2195-T84 Coupons Tensile Testing

2195-T84 (Heat Treated)	YTS(ksi)	UTS(ksi)	Elongation (%)	% Parent Material YTS	% Parent Material UTS
95S1	36.1	37.6	2.8	56	53
95S2	36.7	40.7	3.3	56	57
95S3	39.2	44.9	4.4	60	63
95S4	37.1	38.7	2.5	57	54
95S5	37.1	44.5	3.2	57	63
95S6	38	45.4	4.4	58	64
95S7	37.5	41	3.2	58	58
95S8	38.1	42.1	3.8	59	59
Average:	37.5	41.9	3.5	57	59

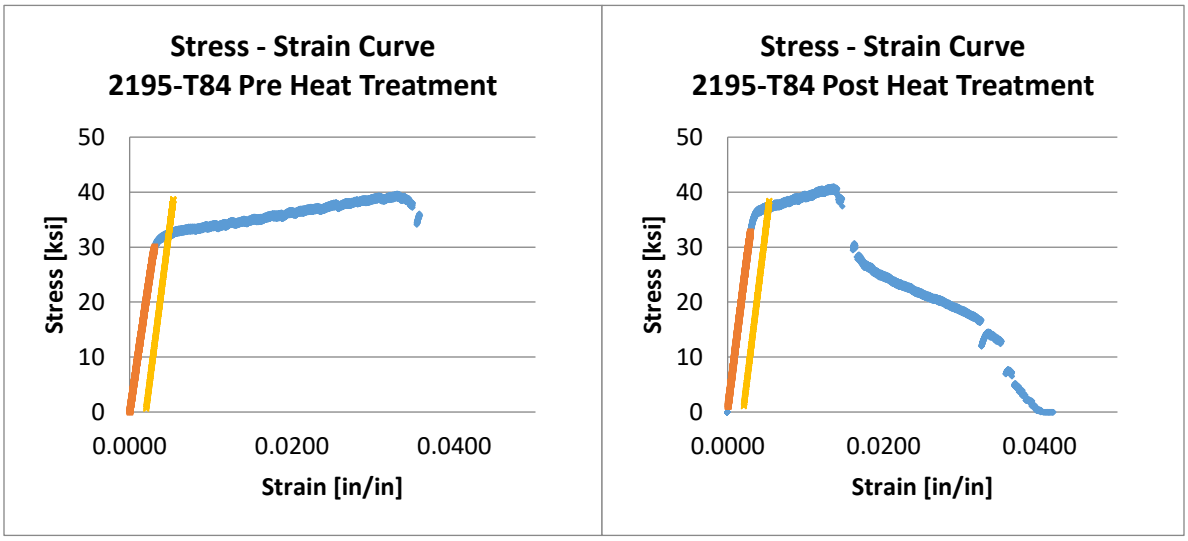

Figure 28: On the left is the representative Stress-Strain Curve of the as welded 2195, while the right is the representative Stress-Strain Curve of the post heat treatment 2195.

Even though no previous work was performed on 2219-T84 with respect to additive friction stir welding, a component was fabricated and heat treatment in the same way as the 2195-T87 to provide a comparison. The tensile testing found that the average YTS over the length of the sample was 29.4 ksi, which is 60% of the parent material YTS. The most surprising result though were the results of the elongation and the UTS. The elongation was found to be 12.8 % on average. In addition to the higher than expected elongation, the coupons had an average UTS of 48.0, which is approximately 91 % of the parent material.

Table 5: Calculated Results of 2219-T84 Tensile Testing

2219-T84 (Heat Treated)	YTS(ksi)	UTS(ksi)	Elongation (%)	% Parent Material YTS	% Parent Material UTS
19S1	29.1	47.7	13.5	59	90
19S2	29.7	47.8	13.6	61	90
19S3	29.4	47.2	13.6	60	90
19S4	29.2	48	11.8	60	91
19S5	28.6	47.4	11.6	58	89
19S6	30	48.9	11.6	61	92
19S7	29.7	48.1	13.9	61	91
19S8	29.8	48.5	12.8	61	92
Average:	29.4	48.0	12.8	60	91

3.5 Discussion and Conclusions

As discussed previously, the purpose of this thesis was to further evaluate the feasibility of Additive Friction Stir Welding (AFSW), assess the potential for and the effectiveness of heat treatment on a set of stacked lap welds, and create a benchmark for further testing. This study has successfully show that this friction stir welding techniques applied to stacked lap welds to create essentially a continuous weld nugget at is a candidate for further study

Based on the results of the testing regiment and the previous work done through the NCAM FSW class, 2195-T84 has shown some potential for use in additive friction stir welding. Even though the yield strength was only around 55% of the parent material in the as welded condition and 58% post heat treatment, the exceptional strength properties of the virgin plates in the short transverse grain direction lead to higher YTS than other Al-Li alloys. Although, several difficulties were encountered with the 2195-T84 throughout the welding process. It was also discovered during the welding process that as the number of stacked welds increases, after approximately four (4) welds, the original weld schedule becomes less effective and the pin tool would gouge the

surface. Although this can be compensated for by increasing the translational speed mid-weld, it appears to have had a negative impact on the final samples, i.e several small voids found in both the macrographic and micrographic images. These types of voids generally originate from excessive travel speeds [22]. If 2195-T84 is to be studied further using similar processes as have been described within, a series of welding schedules should be developed to compensate for this effect.

The second goal was to evaluate the potential for the use of post weld heat treatment to optimize mechanical properties. Results obtained from the simple heat treatment performed were not promising for 2195. A minor increase in the yield strength was observed, but a sizable decrease in the ultimate tensile strength and elasticity make the treatment impractical. Although not many positive results have been found for pure heat treatment of 2195-T84, some promising results have been using various quenching techniques such as fan cooling and water cooling [25, 26, 27]. Any future work with quenching would need to account for warping effects on the weld stack and internal stresses that can occur. Additional results have shown some success with solution treating and aging [23]. It should be noted again that although this heat treatment does not seem to produce positive results for 2195-T84, the as-welded YTS and UTS were still noticeably greater than the values compared to the heat treated 2219-T87.

While the 2195-T84 shows potential for continued study, some of the results of the heat treated 2219-T87 show promise. Even though the initial mechanical properties of 2219-T87 are less favorable than 2195-T84, 2219-T87's weldability and response to heat treatment make it a candidate for further research. Some of the results of the testing do bring up concerns. Without any results of tensile testing in the as welded condition, the Rockwell hardness and Vickers microhardness along with macrographic imagery are only used as a comparison to evaluate the

mechanical properties. The initial Rockwell hardness measurement of 46 ± 2 is only 64% the value of the parent material. This taken along with the lower Vickers microhardness values measured within the weld nugget area, again found to be approximately 61% of the virgin 2219-T87, raise concerns about the as suitability of the as welded condition.

3.6 Further Testing

Little work has been done in been done in Additive Friction Stir Welding, and there are a many options for continued work in the area. Aluminum 2195-T84 has shown potential in the as welded state and has substantial room to improve, both in refining the weld process and discovering the appropriate post weld strengthening process. In contrast, 2219-T87's well established position in FSW, its weldability and its capacity to be improved through heat treatment makes it a good candidate to explore more complicated designs. Again, the weld schedules should be further explored to produce consistent quality welds throughout the entire stack.

This investigation utilized a fixed pin tool with a flared tip and a scrolled shoulder, which served as a functional proof of concept. The fixed pin tool created several issue though including gouging the surface and leaving a large exit hole at the end of each weld. A newer variation of friction stir welding has shown potential for use in AFSW. Static or stationary shoulder friction stir welding utilizes a combination of a pin tool that can rotate high speeds independent of the shoulder that does not rotate, but can apply some force to help with consolidation. This static shoulder drastically reduces the effect of the welding process on the surface of the sample. The high rotational speed of the tool expands the stir zone and is capable of producing a larger weld nugget zone, is advantageous when the final manufactured part will be machined down to the weld nugget [30, 31, 32, 33, 34].

REFERENCES

1. Thomas, W. M., Nicholas, E. D., Needham, J. C., Murch, M. G., Temple-Smith, P., & Dawes, C. J. (1995). *U.S. Patent No. 5,460,317*. Washington, DC: U.S. Patent and Trademark Office.
2. Maryon, H. (1941). 85. Archæology and Metallurgy. I. Welding and Soldering.*Man*, *41*, 118-124
3. Norfolk, M., & Johnson, H. (2015). Solid-state additive manufacturing for heat exchangers. *JOM*, *67*(3), 655-659.
4. Courtesy of Fabrisonic, < http://fabrisonic.com/solutions-for-3d-printing-fluid-channels-part-3/> February, 2016
5. Romine, P. L. (1996). Investigation of Machine Design for Friction Stir Welding.
6. Jones, C., & Adams, G. (1999). Assembly of a full-scale external tank barrel section using friction stir welding.
7. "Final Friction Stir Weld Completed on Orion Spacecraft", <https://www.nasa.gov/mission_pages/constellation/orion/orion_first_weld.html> June 15, 2010
8. Courtesy of NASA < https://www.nasa.gov/centers/marshall/michoud/orion_test_article.html> April, 20, 2009
9. Delany, F., Kallee, S. W., & Russell, M. J. (2007). Friction stir welding of aluminium ships. *Electric Welding Machine*, *6*, 019.
10. Courtesy of marinetraffic.com, <http://www.marinetraffic.com/en/photos/of/ships/shipid:663691/#forward>
11. Pasha, A., Reddy, R., Laxminarayana, P., & Khan, I. A. (2014). INFLUENCE OF PROCESS AND TOOL PARAMETERS ON FRICTION STIR WELDING–OVER VIEW.
12. Brooke, S. A., & Bradford, V. (2012). Friction Pull Plug Welding in Aluminum Alloys..
13. Kaufman, J. G. (2000). *Introduction to aluminum alloys and tempers*. ASM international.
14. Chen, P. S., Kuruvilla, A. K., Malone, T. W., & Stanton, W. P. (1998). The effects of artificial aging on the microstructure and fracture toughness of Al-Cu-Li alloy 2195. *Journal of materials engineering and performance*, *7*(5), 682-690.
15. Pavlina, E. J., & Van Tyne, C. J. (2008). Correlation of yield strength and tensile strength with hardness for steels. *Journal of Materials Engineering and Performance*, *17*(6), 888-893.
16. Zhang, P., Li, S. X., & Zhang, Z. F. (2011). General relationship between strength and hardness. *Materials Science and Engineering: A*, *529*, 62-73.
17. Cahoon, J. R., Broughton, W. H., & Kutzak, A. R. (1971). The determination of yield strength from hardness measurements. *Metallurgical Transactions*, *2*(7), 1979-1983.
18. ASTM E18-16, Standard Test Methods for Rockwell Hardness of Metallic Materials, ASTM International, West Conshohocken, PA, 2016, www.astm.org

19. Chicot, D., Mercier, D., Roudet, F., Silva, K., Staia, M. H., & Lesage, J. (2007). Comparison of instrumented Knoop and Vickers hardness measurements on various soft materials and hard ceramics. *Journal of the European Ceramic Society*, *27*(4), 1905-1911.

20. ASTM E92-16, Standard Test Methods for Vickers Hardness and Knoop Hardness of Metallic Materials, ASTM International, West Conshohocken, PA, 2016, www.astm.org

21. ASTM E8 / E8M-16a, Standard Test Methods for Tension Testing of Metallic Materials, ASTM International, West Conshohocken, PA, 2016, www.astm.org

22. Zhang, H., Wang, M., Zhang, X., Zhu, Z., Yu, T., & Yang, G. (2016). Effect of welding speed on defect features and mechanical performance of friction stir lap welded 7B04 aluminum alloy. *Metals*, *6*(4), 87.

23. Kostrivas, A., & Lippold, J. C. (1999). Weldability of Li-bearing aluminium alloys. *International materials reviews*, *44*(6), 217-237.

24. Oertelt, G., Babu, S. S., David, S. A., & Kenik, E. A. (2001). Effect of thermal cycling on friction stir welds of 2195 aluminum alloy. *Welding journal*, *80*(3), 71-s.

25. Hales, S. J., & Lippard, H. E. (1994). Influence of post-superplastic forming practices on the tensile properties of aluminum-lithium alloys. *Journal of materials engineering and performance*, *3*(3), 334-343.

26. Hales, S. J., & Lippard, H. E. (1993). Effect of thermal processing practices on the properties of superplastic Al-Li alloys.

27. Yoon, J. H., Yoo, J. T., Min, K. J., & Lee, H. S. (2015). A Study on Post Weld Heat Treatment of Friction Stir Welded Al2195 Blank for Spin Forming. In *Advanced Materials Research* (Vol. 1125, pp. 190-194). Trans Tech Publications.

28. Leonard, A. J., & Lockyer, S. A. (2003, May). Flaws in friction stir welds. In *4th international symposium on friction stir welding* (Vol. 16). Park City, Utah, USA.

29. Thomas, W., Nicholas, E. D., Staines, D., Tubby, P. J., & Gittos, M. F. (2006). FSW Process Variants and Mechanical Properties. *WELDING RESEARCH ABROAD*, *52*(4), 12.

30. Li, J. Q., & Liu, H. J. (2013). Effects of tool rotation speed on microstructures and mechanical properties of AA2219-T6 welded by the external non-rotational shoulder assisted friction stir welding. *Materials & Design*, *43*, 299-306.

31. Li, J. Q., & Liu, H. J. (2013). Characteristics of the reverse dual-rotation friction stir welding conducted on 2219-T6 aluminum alloy. *Materials & Design*, *45*, 148-154.

32. Li, Z., Yue, Y., Ji, S., Chai, P., & Zhou, Z. (2016). Joint features and mechanical properties of friction stir lap welded alclad 2024 aluminum alloy assisted by external stationary shoulder. *Materials & Design*, *90*, 238-247.

33. Hassan, K. A., Prangnell, P. B., Norman, A. F., Price, D. A., & Williams, S. W. (2003). Effect of welding parameters on nugget zone microstructure and properties in high strength aluminium alloy friction stir welds. *Science and Technology of Welding and joining*, *8*(4), 257-268.

34. Wu, H., Chen, Y. C., Strong, D., & Prangnell, P. (2014). Assessment of the advantages of static shoulder FSW for joining aluminium aerospace alloys. In *Materials Science Forum* (Vol. 783, pp. 1770-1775). Trans Tech Publications

35. Courtesy of The Welding Institute, < http://www.twi-global.com/technical-knowledge/published-papers/recent-developments-in-friction-stir-welding-of-thick-section-aluminium-alloys-march-2007/>, March, 2007

36. Courtesy of Par Systems, <http://www.par.com/technologies/friction-stir-welding>

37. Fadaeifard, F., Gharavi, F., Matori, K. A., Daud, A. R., Ariffin, M., Anuar, M. K., & Awang, M. (2013). Investigation of microstructure and mechanical properties of friction stir lap welded AA6061-T6 in various welding speeds. *Journal of Applied Sciences*, *14*(3), 221-228.

38. Pham, D., & Dimov, S. S. (2012). *Rapid manufacturing: the technologies and applications of rapid prototyping and rapid tooling*. Springer Science & Business Media.

39. Frazier, W. E. (2014). Metal additive manufacturing: a review. *Journal of Materials Engineering and Performance*, *23*(6), 1917-1928.

40. Gu, D. D., Meiners, W., Wissenbach, K., & Poprawe, R. (2012). Laser additive manufacturing of metallic components: materials, processes and mechanisms. *International materials reviews*, *57*(3), 133-164.

41. Brown Jr., W. F., (1999). Aerospace structural metals handbook. *Purdue Research Foundation, West Lafayette, Indiana*, 2.

42. Beckham, A., Sunderström M. (2014). Development of Stationary Shoulder for Friction Stir Welding (Master's Thesis). Chalmers University of Technology, Gothenburg, Sweden

Vita

Matthew Champagne grew up the youngest of six children in the small city of Houma, near the Gulf coast of Louisiana. In 2006 he graduated summa cum laude from Vandebilt Catholic High School. He continued his education the next semester at Louisiana State University (LSU) after being accepted into the Louisiana Science, Technology, Engineering, and Mathematics (LA-STEM) program. He began his research career under Dr. David Young and Dr. Phillip Adams at the same time he began classes. Four years later, in 2010, Matthew graduated with his BSc in physics. He was then accepted to LSU as a graduate student in physics. After taking a year off from research, he began working under Dr. Phillip Sprunger, learning about both vacuum and surface science. The next summer (2012) he began his thesis project under Dr. Shane Stadler. After successfully defending his thesis in December of the same year, he received his master degree with a concentration in condensed matter physics in May of 2013.

After starting a job working as a geotechnical laboratory technician in February of 2014, Matthew enrolled in the master program in mechanical engineering at the University of New Orleans starting the summer semester of 2014. The fall semester of that same year, at the recommendation of Dr. Paul Schilling, he took the NCAM friction stir welding course taught by Dr. Michael Eller. The course sparked an interest in the friction stir welding (FSW) and manufacturing. In a pursuit of the newly found curiosity, Matthew began working with Dr. Schilling and Dr, Eller as a teaching assistant for the FSW course. He began working on his thesis project the summer of 2015 with both Dr. Schilling and Dr. Eller working as advisers. January of 2016 started his career as a staff scientist for Professional Services Industries (PSI) working as a geotechnical project manager. After successfully defending his thesis in August of 2017, he will receive his master degree in engineering concentrating in mechanical engineering in December 2017.